

Phase transformations of continental crust during subduction and exhumation: Western Gneiss Region, Norway

EMILY M. PETERMAN^{1,2,*}, BRADLEY R. HACKER¹ and ETHAN F. BAXTER³

¹ Department of Earth Science, University of California, Santa Barbara, Santa Barbara, CA 93106-9630, USA

² now at: Department of Earth and Planetary Sciences, University of California, Santa Cruz,
Santa Cruz, CA 95064, USA

*Corresponding author, e-mail: peterman@ucsc.edu

³ Department of Earth Sciences, Boston University, 685 Commonwealth Avenue, Boston, MA 02215, USA

Abstract: Whether quartzofeldspathic rocks transform to (U)HP minerals during subduction – and back to low-pressure minerals upon exhumation – remains one of the more profound questions pertaining to collisional orogenesis. Garnet-bearing quartzofeldspathic gneisses from the Western Gneiss Region, Norway provide an opportunity to answer this question. High-precision Sm-Nd garnet geochronology of these gneisses documents garnet growth from 418 to 398 Ma. Garnet zoning in two samples implies growth during subduction-related increase in pressure from 0.5 GPa and 550 °C to 1.7 GPa and 700 °C. Zoning in all other garnets suggests growth over rather narrow *P–T* ranges from 1.0–1.6 GPa and 725–800 °C during decompression, possibly accompanying melting. If these samples constitute a representative suite, (i) the dearth of (U)HP garnets suggests that most of the quartzofeldspathic gneisses in the Western Gneiss Region did not transform to eclogite-facies parageneses during subduction; (ii) the abundance of garnets grown during decompression indicates that the major period of densification was during exhumation. The widespread metastability of quartzofeldspathic rocks during subduction is substantially different from the findings of previous work and suggests commensurately less subduction of continental crust before the slab is positively buoyant.

Key-words: UHP metamorphism, Western Gneiss Region, symplectite, garnet, Sm-Nd, *Perple_X*, continental crust, phase transformations, subduction, exhumation.

1. Introduction

Over the past two decades, researchers have established that ultrahigh-pressure (UHP) metamorphism of continental crust is not rare, but instead plays a fundamental role in the evolution of collisional orogens (Ernst, 2001). The presence of coesite in eclogite demonstrates that some mafic rocks transform to eclogite at UHP conditions, but eclogites are typically minor inclusions in quartzofeldspathic gneiss that itself usually lacks evidence of high-pressure minerals. This prompts the following questions: *Does subducted quartzofeldspathic gneiss typically transform at (ultra)high pressure? What are the geodynamic implications of the phase transformations that take place in continental crust during subduction and exhumation?*

The high- and ultrahigh-pressure Western Gneiss Region (WGR) of Norway is an ideal setting in which to investigate these questions because the gneisses contain widespread garnet, which can yield information about the age of metamorphism and the pressure and temperature conditions recorded by the rock. Data from these garnet-bearing lithologies illuminate the phase transformations

and attendant changes in density and rheology experienced by subducting and exhuming continental crust.

This paper first presents Sm-Nd geochronology that dates garnet growth in quartzofeldspathic gneisses. Second, modeling of compositional zoning in garnet is used to constrain the pressures and temperatures of garnet growth. These data suggest that the bulk of the WGR quartzofeldspathic gneiss was subducted and exhumed without undergoing wholesale transformation to *eclogite-facies* minerals. This paper finally discusses how this conclusion affects our understanding of the density of subducted crust, the global geochemical cycle and the rheology of continental crust.

2. Geologic background

2.1. Evidence and role of UHP metamorphism in collisional orogenesis

It is now known that (U)HP metamorphism can occur several times during the evolution of a single orogen

(Brueckner & van Roermund, 2004), that episodes of continental subduction and exhumation can last from 5 to 30 Myr (Hacker *et al.*, 2006; McClelland *et al.*, 2006; Mattinson *et al.*, 2007; Kylander-Clark *et al.*, 2008; Spengler *et al.*, 2009) and that UHP bodies can be exhumed from the mantle as thick, coherent slabs (Hacker *et al.*, 2000; Kylander-Clark *et al.*, 2008), and, possibly, as thin sheets (Ernst, 2006). Much of the work conducted on UHP terranes has focused on eclogites because they retain the most information about the maximum pressures and temperatures attained during orogenesis (Cuthbert *et al.*, 2000).

Though eclogites provide direct evidence of mineralogical transformation at UHP, mafic bodies comprise <5 vol% UHP terranes. Although continental crust can transform to (U)HP minerals (Carswell & Cuthbert 1986; Dewey *et al.*, 1993), the paucity of quartzofeldspathic gneisses with (U)HP phases and the abundance of amphibolite-facies minerals suggests otherwise (Dransfield 1994). Alternatively, the absence of (U)HP phases may indicate that eclogitized continental crust completely back-reacts to low-pressure phases or does not return to the surface.

Previous studies have highlighted rocks that remained metastable throughout subduction to (ultra)high pressures (Wain 1997; Krabbendam *et al.*, 2000; Wain *et al.*, 2001). That dry coarse-grained crustal rocks can survive burial to pressures as high as 3 GPa at temperatures in excess of 700 °C without wholly transforming to denser minerals (Austrheim, 1987; Austrheim *et al.*, 1997; Straume & Austrheim, 1999; Engvik *et al.*, 2000; Krabbendam *et al.*, 2000), indicates that phase transformations require fluid, fine grain size, deformation or some other energy source. Such studies demonstrate that phase transformations cannot be presumed *a priori* to follow equilibrium and that kinetics play an important role in the rate and/or occurrence of these reactions. Despite the lack of widespread evidence for densification of quartzofeldspathic rocks at UHP, geodynamic models have generally assumed mineralogical transformation of the crust *in toto* (Gerya & Stöckhert, 2006; Warren *et al.*, 2008a and b; Yamato *et al.*, 2008). Particularly important for modeling, the degree to which continental crust transforms during UHP subduction affects 1) the body forces attending subduction and exhumation, 2) the rheology of the crust, and 3) the mode of exhumation of the UHP terrane.

Most rocks in UHP terranes – especially non-mafic rocks – lack (U)HP phases and are composed of amphibolite-facies minerals that formed at 1.5–0.5 GPa during exhumation after the UHP event (Zhang *et al.*, 1995; Banno *et al.*, 2000; Krabbendam *et al.*, 2000; Nakamura & Hirajima, 2000; Walsh & Hacker, 2004). In the Dabie–Sulu terrane, for example, the only direct evidence of UHP metamorphism in the bulk gneiss is rare occurrences of coesite, polycrystalline quartz (PCQ) after coesite, and diamond – mostly as inclusions in other minerals (Wang & Liou, 1991; Wang *et al.*, 1992; Okay, 1993; Cong *et al.*, 1995; Liu & Liou, 1995; Tabata *et al.*, 1998). In the UHP Northeast Greenland Caledonides, evidence of UHP metamorphism of the gneiss that hosts the eclogites is limited to a few polycrystalline quartz inclusions in

garnet-bearing gneisses (Gilotti & Krogh Ravna, 2002). In the Western Gneiss region of Norway, evidence of UHP metamorphism in the quartzofeldspathic gneiss is restricted to a few locations with diamond (Dobrzhinetskaya *et al.*, 1995) and quartz pseudomorphs after coesite in garnet and clinzoisite (Wain, 1997). Quartzofeldspathic gneisses with (U)HP matrix minerals – such as kyanite, phengite, zoisite, and garnet (Austrheim, 1987; Koons *et al.*, 1987; Black *et al.*, 1988; Hacker, 2008) – are restricted to rare domains, generally interlayered with eclogite (*e.g.* Wain, 1997; Cuthbert *et al.*, 2000); the bulk of the quartzofeldspathic gneisses in UHP terranes are composed of amphibolite-facies minerals.

The absence of (U)HP phases in quartzofeldspathic gneisses may simply be the result of strong overprinting by subsequent metamorphic events. Overprinting is expected in quartzofeldspathic rocks because the stability of hydrous phases (*e.g.* phengite) decreases during decompression, causing fluid release – and possibly melting (Vielzeuf & Holloway, 1988) – that facilitates re-equilibration (Heinrich, 1982).

2.2. The Western Gneiss Region, Norway

Because of its geographic extent (>30,000 km² of HP and ~5,000 km² of UHP rocks) and excellent exposure, the Western Gneiss Region (WGR) of Norway is an ideal location in which to investigate UHP processes (Fig. 1). Mafic bulk compositions comprise ~2 vol% of the WGR. In the southern and eastern WGR (Fig. 1), these rocks show incipient eclogitization and variable retrogression to amphibolite-facies minerals. Eclogite-facies recrystallization of mafic rocks intensifies to the northwest, culminating in four domains with UHP eclogites in the coastal region of the study area.

Although it contains mafic bodies, the WGR is predominantly composed of amphibolite-facies quartzofeldspathic gneiss called the Western Gneiss Complex (WGC). The main lithology in the WGC (~70 vol%) is biotite ± hornblende ± garnet granodiorite–tonalitic gneiss with 5–80 % (typically 20–40 %) cm-scale granitic leucosomes (Bryhni, 1966). Garnet is present in roughly one-third of the WGC gneiss. This gneiss grades with increasing K-feldspar abundance into biotite granitic gneiss that underlies ~10 % of the study area, and with increasing muscovite into two-mica tonalitic gneiss that comprises ~5 %. Thermobarometric estimates of the equilibration conditions of minor but widespread garnet-bearing pelites and amphibolites in the WGC range from 650–800 °C and ~0.5–1.5 GPa; thin-section textures such as the presence of cordierite, and sillimanite overprinting kyanite require decompression (Wilks & Cuthbert, 1994; Hacker *et al.*, 2003; Schärer & Labrousse, 2003; Walsh & Hacker, 2004; Root *et al.*, 2005).

The WGC is overlain by allochthons of oceanic and continental affinity. The allochthons were emplaced, metamorphosed and deformed in the early phases of the Caledonian orogeny from ~435 to 420 Ma (Gee, 1975). Later stages of this orogeny, termed the Scandian, were

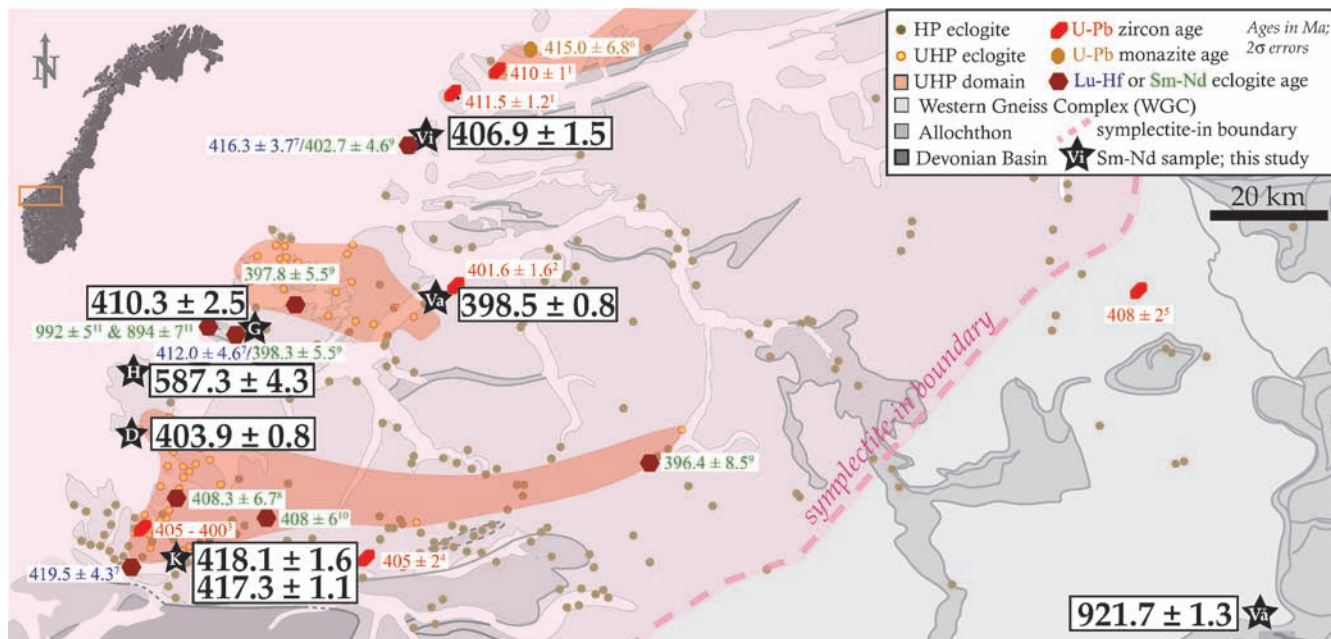


Fig. 1. Western Gneiss Region of Norway (WGR). Stars indicate dated samples: Vi – Vigra, Va – Vartdal, G – Gurskøy, H – Honningsvåg, D – Drage, K – Kroken, Vå – Vågåmo. The eastern limit of symplectite in gneiss is marked by the “symplectite-in boundary.” Superscripts to ages: U-Pb zircon 1) (Krogh *et al.*, 2004); 2) (Carswell *et al.*, 2003b); 3) (Root *et al.*, 2004); 4) (Young *et al.*, 2007); 5) (Kylander-Clark *et al.*, 2006); U-Pb monazite 6) (Terry *et al.*, 2000); Lu-Hf eclogite 7) (Kylander-Clark *et al.*, 2007). Sm-Nd eclogite 8) (Carswell *et al.*, 2003a); 9) (Kylander-Clark *et al.*, 2007); 10) (Mearns, 1986); 11) (Root *et al.*, 2005).

responsible for the subduction of the WGR to >100 km depth from 420 to 400 Ma (Kylander-Clark *et al.*, 2007), and subsequent exhumation to shallow crustal levels where a regionally extensive amphibolite-facies overprint occurred from 400 to 385 Ma (Hacker & Gans, 2005; Kylander-Clark *et al.*, 2008). These events are the latest in the complex polymetamorphic history of the WGR, which includes several magmatic and orogenic events between 1700 and 1250 Ma (Gaál & Gorbatshev, 1987) and a ~930–900 Ma granulite-facies metamorphism (Root *et al.*, 2005; Bingen *et al.*, 2008; Glodny *et al.*, 2008).

2.3. Phase transformations in the Western Gneiss Region

Whether a rock transforms to a high-pressure mineral assemblage depends on a range of factors, including bulk composition, fluid activity, grain size, mineralogy, deformation, *etc.* These factors varied across the WGR, leading to a range of transformation behaviors during and after subduction. Perhaps the simplest of these factors to consider is bulk composition.

Most (~85 %) of the WGC is composed of quartzofeldspathic gneiss with an amphibolite-facies mineralogy that locally includes garnet. In the eastern third of the WGC, the gneiss hosts HP eclogite blocks, but is composed almost exclusively of coarse amphibolite-facies minerals and has titanite with Precambrian U-Pb ages (Kylander-Clark *et al.*, 2008). These features suggest that, in the east, the gneiss did not transform to eclogite-facies

minerals; if it had, the titanite should be replacing Scandian rutile. In contrast, the western two-thirds of the WGC contains eclogite blocks (about a dozen of which have coesite or polycrystalline quartz (PCQ) after coesite) and titanite with Scandian U-Pb ages. These factors suggest that the gneiss in the west transformed to high-pressure minerals during subduction and then back to amphibolite-facies minerals afterward; below we offer the interpretation that much of this gneiss did in fact not transform to high-pressure minerals.

Approximately 25 % of the quartzofeldspathic gneiss in the WGR contains mm- to cm-scale garnet in abundances up to ~17 % (typically a few percent or less). Labrousse *et al.* (2004) calculated metamorphic conditions of 1.1–1.4 GPa, ~700°C for two such garnet-bearing gneisses; these conditions are compatible with those determined for pelites and amphibolites in the WGC (see above). Sm-Nd geochronology of one 15 cm garnet gave a Precambrian age (Root *et al.*, 2005). Walsh & Hacker (2004) and Schärer & Labrousse (2003) assumed that the garnets grew during the post-UHP amphibolite-facies overprint, but did not conduct geochronology to determine the timing of garnet growth.

Precisely when and how garnets grew in different rocks in the WGR is important to understand because the formation of garnet is the single biggest density change a quartzofeldspathic rock is likely to experience during subduction to depths of <200 km (Massonne, 2008). Numerous studies have shown that coarse-grained rocks do not necessarily undergo mineralogical transformations – even at pressures as high as 3 GPa and temperatures as high as 750 °C – if a critical catalyst, such as H₂O or deformation, is missing

(Rubie, 1986; Austrheim, 1987; Hacker, 1996; Austrheim, 1998; Krabbendam *et al.*, 2000; Baxter, 2003; John & Schenk, 2003). If disequilibrium at such conditions is a general feature of Earth, it has important implications for the rates and mechanics of plate tectonics.

There are at least four different histories that can explain the presence of garnet in the amphibolite-facies quartzofeldspathic gneisses of the WGR (Fig. 2):

- (A) Garnet is a relict phase from an earlier, *e.g.*, Precambrian, metamorphism. The minerals in the rock were metastable during subduction and underwent minimal Caledonian recrystallization.
- (B) Garnet grew along the prograde path during subduction and was preserved metastably during

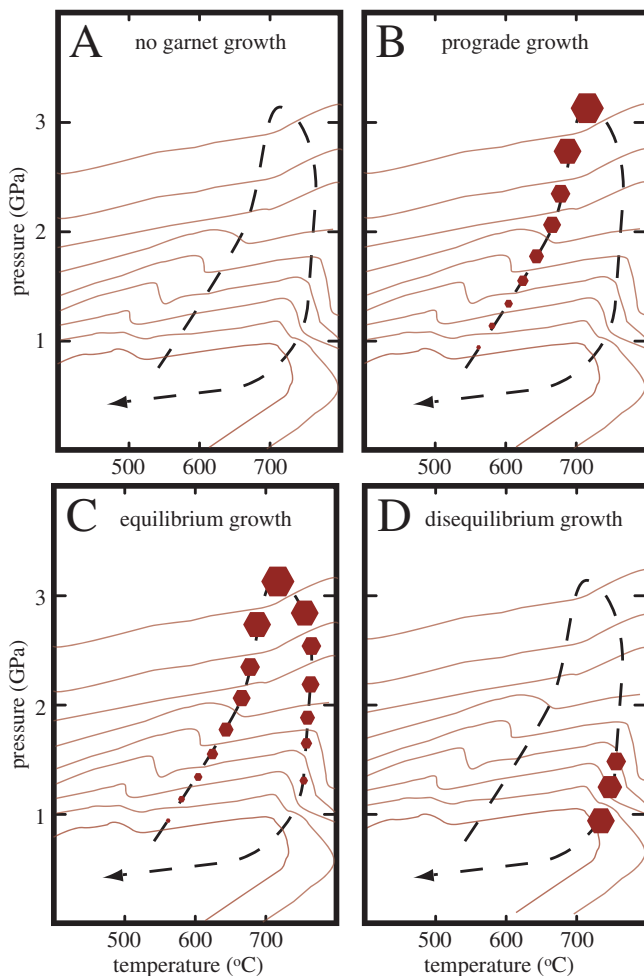


Fig. 2. P - T path shown as a dashed line; schematic contours show increasing garnet volume under equilibrium conditions. End-member garnet growth histories: A) No garnet grows during subduction or exhumation. B) Garnet grows exclusively along the prograde path. C) Garnet grows along the prograde path and is then consumed during decompression. D) Garnet grows during decompression, not during prograde metamorphism. If A, garnet should be Precambrian. If B, garnet should be Caledonian and preserve prograde compositional zoning. If C, garnet should be Caledonian with sharp increase in Mn content at the rims as a result of resorption. If D, garnet should be Caledonian with compositions that suggest a narrow window of P - T conditions.

decompression and exhumation. Other minerals in the rock reacted during subduction, but underwent minimal subsequent recrystallization.

- (C) Garnet grew along the prograde path during subduction and was partially consumed during decompression and exhumation. Other minerals in the rock reacted during both subduction and exhumation.
- (D) Garnet grew only during exhumation; other minerals in the rock reacted at the same time.

The four scenarios above represent end-member possibilities – modifications or combinations of these are also possible. Differentiation among these hypotheses may be possible by combining garnet geochronology with garnet petrology. If hypothesis A is correct, garnet will yield a pre-subduction age (*e.g.*, ~ 1.6 to 0.9 Ga), and the garnet composition and its mineral inclusions should reflect growth at non-(U)HP conditions. If hypothesis B is correct, garnet should yield an age of ~ 420 to 400 Ma – similar to eclogite ages – and zoned garnets and minerals included in garnet should reflect rimward increases in pressure and temperature. If hypothesis C is correct, zoned garnets and their inclusions will reflect prograde growth followed by resorption; evidence of the latter may include rim enrichment in Mn and xenoblastic garnet surrounded by biotite + plagioclase + quartz (Auzanneau *et al.*, 2006). If hypothesis D is correct, the garnet will be younger than the (U)HP metamorphism (~ 400 to 390 Ma, based on the ages of post-UHP titanite (Kylander-Clark *et al.*, 2008)). If present, compositional zoning will reflect growth at low pressure. Garnet geochronology and compositional zoning presented in the following sections show which growth histories best explain the garnet-bearing gneisses in the Western Gneiss Region.

The remaining 15 % of the Western Gneiss Complex that is not quartzofeldspathic gneiss includes mafic rocks, coarse-grained biotite-rich seams within quartzofeldspathic gneiss, K-feldspar augen gneiss, Precambrian granulite-facies gneisses and ‘quartzite’ layers:

- Mafic rocks represent ~ 2 % of the WGC. Eclogite-facies minerals in these rocks prove transformation at (U)HP.
- Coarse-grained biotite-rich seams within the quartzofeldspathic gneiss constitute ~ 5 % of the WGC. Phase diagram calculations with *Perple_X* (Connolly & Petri, 2002) indicate that this same mineral assemblage is stable at (U)HP conditions and therefore will show no mineralogical record of subduction.
- Another 5 % of the WGC is composed of K-feldspar augen gneiss. Phase diagram calculations with *Perple_X* indicate that these bulk compositions should contain 1 vol% garnet at ~ 1 GPa and 2.5 vol% garnet at 3 GPa in equilibrium with jadeitic clinopyroxene and phengite. The coarse grain size and the absence of garnet, clinopyroxene and phengite are compatible with either a lack of reaction at (U)HP or wholesale back-reaction after subduction.
- Relict Precambrian granulite-facies rocks that did not transform to eclogite-facies minerals make up ~ 1 % of the WGC (Wain *et al.*, 2001). There were

presumably some granulite-facies rocks that transformed during subduction or exhumation, but their volume fraction is unknown.

- Quartzite layers comprise ~1 % of the WGC. These layers may have transformed to coesitite and subsequently retrogressed wholesale during exhumation, but there are no data to evaluate this.

3. Sm-Nd geochronology

3.1. Analytical methods

3.1.1. Whole-rock dissolution

Approximately 50 g of each sample were ground in agate to <50 μm . A 100–150 mg aliquot of each sample was weighed and transferred into a 15 mL Savillex screw-top beaker for digestion in 1:1 29 N HF and 1.5 N HCl for 24–48 h at 130 °C. Once digested, the samples were dried and re-dissolved in 1:1 ratio of 7 N HNO₃ and 1.5 N HCl. The samples were then covered and placed on a hot plate at 130 °C overnight to break down fluoride salts. Finally, the samples were dried and re-dissolved in ~5 mL 1.5 N HCl. An aliquot of each sample equivalent to 300 ng of Nd was spiked with ¹⁴⁷Sm–¹⁵⁰Nd prior to column chemistry.

3.1.2. Garnet dissolution

To yield ~20–100 mg separates of garnet, ~500 g of each sample were crushed and sieved to 120–240 μm . Garnet grains were separated with heavy liquids and a Frantz Isodynamic magnetic separator and then picked by hand. Only monocrystalline fragments that were free of visible inclusions were selected for analysis. The garnet separates were initially cleaned overnight at 130 °C with 5 mL 1.5 N HCl in a 15 mL Savillex screw-top beaker to remove picking contaminants and dissolve phosphate minerals. The HCl was decanted and the garnets were then rinsed and ultrasonicated in Milli-Q water twice. Seven of the eight garnet samples (excluding the Gurskøy sample) were then further cleansed of microscopic inclusions using a partial dissolution procedure similar to Baxter *et al.* (2002). Crushed garnet samples were treated with a 1:1 ratio of 29 N HF and 1.5 N HCl at 110 °C for 45 min in a covered 15 mL Savillex screw-top beaker. The HF + HCl solution was decanted and the garnets were rinsed and ultrasonicated twice in 1.5N HCl and then twice in Milli-Q water; the liquid was decanted after each ultrasonication. To remove the fluorides that formed during the HF treatment, the garnet fractions were dried after the final Milli-Q decant step and brought up in 1 mL each of 1.5 N HCl and HClO₄. The samples were covered and heated at 130 °C for 3 h and then left uncovered overnight to dry. An additional 500 μL of 1.5 N HCl was added to each sample and decanted to rinse HClO₄ and re-precipitated solid residues off the grains. Each sample was then dried and re-measured to determine the final mass of cleansed garnet to be dissolved for analysis.

The garnet samples were dissolved in a 1:1 solution of 29 N HF and 1.5 N HCl at 130 °C. Garnets were completely dissolved in 12–90 h, depending on grain size and quantity of sample. To break down the fluoride salts that formed during garnet dissolution, 2 mL each of concentrated HNO₃ and HCl were added to the samples, which were then heated for 12–36 h at 130 °C. After complete dry-down, samples were brought up in ~5 mL 1.5 N HCl.

A 1 mg aliquot of each garnet sample was spiked with ¹⁴⁷Sm–¹⁵⁰Nd and run as a “mixed spike” on the TIMS to obtain approximate concentrations of Sm and Nd; these concentrations were used to determine the amount of spike required for the remaining garnet fractions. Following mixed-spike analysis, all samples were spiked and run through ion-exchange separation column chemistry.

3.1.3. Column chemistry and isotopic measurements

Whole-rock and garnet fractions were run through two sets of ion-exchange separation column chemistry following Harvey and Baxter (2009). Samples first passed through TRU-spec columns executed with 0.05 N and 2.0 N HNO₃ to isolate rare-earth elements. Samples were then loaded onto cation exchange columns in 0.75 N HCl. Samarium and Nd isotopes were collected using 0.2 N methylactic acid with a pH of 4.67. Following an overnight dry-down under a heat lamp, 100 μL of concentrated HNO₃ were added to each sample twice to remove organic material. Procedural blanks were run with each set of columns to establish the background levels of Sm and Nd, and to identify and correct for any interferences on the targeted Sm and Nd isotopes.

Isotopic measurements were collected on a ThermoFinnigan Triton TIMS at Boston University following the methods of Harvey & Baxter (2009). Neodymium was analyzed as NdO⁺ using single Re filaments. Samples were loaded in 1 μL 2N HNO₃ and 2 μL of a Ta₂O₅ slurry in H₃PO₄ to improve NdO⁺ yield. Filament current was adjusted to maintain a ¹⁴²Nd¹⁶O signal of 1–2 V for whole rock analyses and 0.3–0.5 V for garnet analyses. After the work was completed, we learned that some Nd had been lost during column chemistry (due to swamping of TRU-spec columns by abundant Fe in garnet), thereby reducing the actual load sizes and beam sizes of garnet Nd analyses (see Harvey & Baxter, 2009). Typically, 200–1000 cycles were collected per analysis, depending on the size of the Nd load and stability of the beam. Neodymium isotope ratios were fractionation corrected using an exponential law to ¹⁴⁶Nd/¹⁴⁴Nd = 0.7219. Samarium samples were loaded onto a double filament in 1 μL 2N HNO₃; the filament current was adjusted to maintain a signal of 0.5–1.2 V, with 500–1000 cycles collected per analysis. Repeat analyses of an in-house Nd isotopic standard (Ames metal) over nine months yielded 0.512131 ± 0.000010 (2 σ standard deviation; $n = 83$). Within-barrel precision (applicable to garnet–whole rock pairs run in the same barrel) was 0.512130 ± 0.000007 (2 σ standard deviation; $n = 19$).

3.2. Sample descriptions

Seven garnet + biotite ± hornblende ± K-white mica quartzofeldspathic gneisses were selected for Sm-Nd geochronology based on geologic context and garnet texture. Six of the seven garnet-bearing samples define a NE-SW transect that crosses two UHP domains in the WGR (Fig. 1); the seventh sample lies at the easternmost extent of the WGR. The sample compositions range from tonalitic to granitic to quartz monzonitic to monzogranitic (Tables 1 and 2). The *P-T* histories of these samples are discussed in Section 4.2. Garnet, plagioclase, biotite and K-white mica compositions were measured on the UCSB Cameca SX50 electron microprobe using a 15 kV accelerating voltage and a 15 nA sample current.

The Kroken paragneiss (Fig. 3a) is composed of garnet (17 vol% determined by point counting) + K-white mica (3.2–3.4 Si atoms per formula unit (p.f.u.)) + plagioclase + biotite. The garnet cores are $\text{prp}_{13}\text{alm}_{71}\text{grs}_{08}\text{sps}_{08}$, 2 mm in radius and contain micrometer to tens-of-micrometers-scale K-white mica + biotite + rutile inclusions; they are mantled by a 1–2 mm zone of $\text{prp}_{18}\text{alm}_{66}\text{grs}_{14}\text{sps}_{02}$ with abundant quartz inclusions, and rimmed by 2–3 mm of inclusion-free $\text{prp}_{26}\text{alm}_{54}\text{grs}_{19}\text{sps}_{01}$ garnet (Fig. 3). Each of these three garnet domains is idioblastic, suggesting limited resorption. The cores of the garnets are pale red in thin section and enriched in Fe and Mn; the rims are pale pink and enriched in Mg and Ca. This color difference allowed the cores and rims to be dated separately. K-white mica is partially broken down to biotite (2.0–2.4 wt% TiO_2); oligoclase (An_{22}) and biotite (1.0 wt% TiO_2) are retrograde phases presumably formed by K-white mica + garnet + albite breakdown.

The Drage monzogranitic gneiss (Fig. 3b) contains K-white mica with high Si cores (3.1–3.3 Si atoms p.f.u.) and muscovite rims (3.0–3.1 Si atoms p.f.u.) + garnet (2 vol%) + rutile + zoisite + oligoclase (An_{22-30}) + biotite (1.6–3.0 wt% TiO_2). Most garnet grains measure 2 mm and are $\text{prp}_{18}\text{alm}_{62}\text{grs}_{19}\text{sps}_{01}$; a few larger (~4 mm) grains

have the same composition. K-white mica occurs in the matrix and as garnet inclusions. Rutile is also included in garnet. K-white mica and garnet have partially broken down to plagioclase and biotite. A polycrystalline quartz inclusion in one of the garnets suggests the former presence of coesite. The rims of ~20 % of the biotite grains are altered to chlorite.

The easternmost HP sample – Vågåmo (Fig. 3c) – is a garnet (2 vol%) + biotite + K-white mica (3.2–3.3 Si atoms p.f.u.) + titanite + rutile tonalitic gneiss. The 1–2 mm garnets are $\text{prp}_{01}\text{alm}_{45}\text{grs}_{45}\text{sps}_{09}$, and are fractured and resorbed, breaking down to magnetite + biotite (0.03 wt% TiO_2) + albite (An_{06-10}). Tens of micrometer- to mm-scale albite and quartz constitute the bulk of the sample; abundant micrometers-scale zoisite spicules overgrow the albite. Titanite and rutile are present in the matrix.

The Vartdal (Fig. 3d) monzogranitic gneiss consists of garnet (15 vol%) + biotite + andesine (An_{12-37} ; mostly An_{32}) + quartz + K-white mica (3.2–3.4 Si atoms p.f.u.) + rutile + zircon. The garnet cores are $\text{prp}_{21}\text{alm}_{48}\text{grs}_{23}\text{sps}_{07}$; the rims are $\text{prp}_{25}\text{alm}_{48}\text{grs}_{24}\text{sps}_{03}$. Garnet ranges in size from ~500 μm to 5 mm. There are two types of biotite: coarse-grained idioblasts (2.2–2.7 wt% TiO_2) in textural equilibrium with garnet, and fine-grained biotite (2.8–4.0 wt% TiO_2) in symplectite with plagioclase formed from the breakdown of garnet + K-white mica + (presumably) sodic plagioclase (Fig. 3d). Plagioclase is also a coarse-grained matrix phase. K-white mica and rutile inclusions are abundant in garnet cores, and the garnets have been partially resorbed. Micrometer-scale K-white mica is included in a few quartz grains. Many K-white mica grains – both within the garnet and in the matrix – are partially decomposed to biotite.

The Honningsvåg sample (Fig. 3e) is a garnet (4 vol%) + hornblende + biotite (1.5–2.5 wt% TiO_2) + andesine (An_{31-42}) + quartz granitic gneiss. Garnet cores are $\text{prp}_{13}\text{alm}_{57}\text{grs}_{20}\text{sps}_{10}$, and riddled with quartz, plagioclase and biotite inclusions; hornblende and

Table 1. Whole-rock data for quartzofeldspathic gneiss from the Western Gneiss Region, Norway.^a

Sample # UTM	Vigra P68017A2 0348107 6940435	Gurskøy 8815G6 0319906 6907793	Honningsvåg P6806A3 0301171 6902297	Drage P6807G 0302307 6891321	Vågåmo P6808D2 0490508 6858407	Vartdal P5627I5 0350761 6912822	Kroken P6805A2 0307630 6870035
SiO ₂	63.37	59.81	65.16	68.27	71.86	67.15	59.50
Al ₂ O ₃	14.64	16.97	15.40	16.17	14.88	13.92	20.47
TiO ₂	1.18	1.03	0.55	0.76	0.35	0.62	1.00
FeO	7.58	7.16	6.38	5.22	2.82	6.62	6.70
MgO	2.17	0.93	3.21	1.93	0.77	3.34	3.24
MnO ^b	0.15	0.22	0.26	0.09	0.08	0.39	0.23
CaO	4.03	4.14	4.14	1.98	3.85	3.26	2.53
Na ₂ O	2.59	3.89	3.00	2.18	4.23	1.99	2.44
K ₂ O	3.85	5.46	1.81	3.23	1.07	2.53	3.77
H ₂ O	1.0	1.0	2.0	1.5	1.0	1.0	1.8

^a Analysis performed by ICP-MS at Washington State University. Values in wt%.

^b MnO excluded from *Perple_X* models.

Table 2. Trace-element data for garnet-bearing quartzofeldspathic gneisses from the Western Gneiss Region, Norway

Concentration ^a (ppm)							
Sample ^b	Vigra	Gurskøy	Honningsvåg	Drage	Vågåmo	Vartdal	Kroken
Sample #	P68017A2	8815G6	P6806A3	P6807G	P6808D2	P5627I5	P6805A2
UTM coordinates	<i>0348107</i>	<i>0319906</i>	<i>0301171</i>	<i>0302307</i>	<i>0490508</i>	<i>0350761</i>	<i>0307630</i>
	<i>6940435</i>	<i>6907793</i>	<i>6902297</i>	<i>6891321</i>	<i>6858407</i>	<i>6912822</i>	<i>6870035</i>
Ba	1032.1	2014.3	462.0	618.6	179.2	358.1	496.1
Cr	36	8	12	68	11	97	82
Cs	2.4	0.3	3.0	1.6	4.8	2.5	2.6
Cu	15	11	88	15	3	2	11
Ga	18	18	19	21	15	18	27
Hf	11.5	34.7	4.4	7.8	2.6	2.9	7.7
Nb	16.9	18.3	6.4	20.1	4.2	7.2	22.6
Ni	16	2	31	21	2	57	61
Pb	15.8	16.6	15.9	11.3	23.8	5.2	16.5
Rb	119.4	64.4	68.1	97.2	64.4	80.1	118.5
Sc	20.8	35.9	20.8	14.1	9.0	18.5	20.8
Sr	252.0	367.0	354.0	120.9	283.6	83.4	115.4
Ta	0.9	0.8	0.4	1.3	0.4	0.5	1.5
Th	5.5	2.2	32.5	16.7	3.8	18.1	19.1
U	1.3	0.6	1.7	1.6	2.3	1.4	1.2
V	110	22	98	73	40	121	157
Y	45.7	52.8	22.9	27.8	26.8	19.4	44.8
Zn	106	100	64	82	36	71	81
Zr	442.9	1914.2	149.8	293.9	92.5	104.6	274.5
La	53.6	56.3	111.8	16.7	15.7	34.4	54.3
Ce	117.3	121.6	212.4	42.0	36.7	75.7	116.4
Pr	14.2	16.3	22.0	4.8	4.3	8.8	13.1
Nd	56.7	68.5	72.8	18.3	17.0	33.7	47.3
Sm	11.2	14.1	11.1	4.1	3.8	6.4	8.9
Eu	2.5	5.9	1.4	1.1	0.8	1.4	1.8
Gd	9.9	12.4	8.0	4.4	3.6	4.9	7.3
Tb	1.2	1.9	1.0	0.8	0.7	0.7	1.3
Dy	9.1	11.2	5.3	5.3	4.5	3.9	8.4
Ho	1.8	2.2	0.9	1.1	1.0	0.8	1.7
Er	4.8	6.0	2.1	3.0	3.2	2.1	4.5
Tm	0.7	0.9	0.3	0.5	0.5	0.3	0.7
Yb	3.9	5.7	1.5	2.9	3.7	1.9	4.1
Lu	0.6	1.0	0.2	0.5	0.6	0.3	0.6

^a Analysis performed by ICP-MS (Ba, Cs, Hf, Nb, Pb, Rb, Sc, Sr, Ta, Th, U, Y, and REE) or X-ray fluorescence (italics) at Washington State University. Data reduction followed Knaak & Hooper (1994) and Johnson *et al.* (1999).

^b For sample locations, see Fig. 1.

biotite are present along grain boundaries and cracks. One garnet retains a K-white mica inclusion. The 0.2–2 mm garnets have broken down extensively to hornblende + biotite + plagioclase. Matrix plagioclase and quartz are present.

The Gurskøy quartz monzonitic gneiss (Fig. 3f) contains mm-scale garnet (13 vol%), biotite (2.2 wt% TiO₂), hornblende and oligoclase (An_{15–28}) with minor quartz and abundant matrix titanite. Garnet (prp₀₅alm₆₈grs₂₃sp₈₀₄) is partially broken down to plagioclase + biotite + hornblende. Both rutile and biotite are included in the garnet cores, but rutile is not a matrix mineral. Amphiboles are coarse, measuring ~500 µm. Garnet-rich (~35 vol%) layers alternate at the cm-scale with hornblende rich (~60 vol%) layers.

The Vigra granitic gneiss (Fig. 3g) consists of garnet (5 vol%) + hornblende + biotite (3.2–4.4 wt% TiO₂) +

oligoclase (An_{21–36}) + scapolite + K-feldspar + titanite. The 200 µm to 500 µm scale garnets are partially decomposed to biotite + plagioclase + hornblende, and have ~20–50 µm biotite inclusions. Garnet cores are prp₁₂alm₅₄grs₂₄sp₁₀; rims are prp₁₀alm₅₂grs₃₄sp₀₄. Plagioclase is also present as matrix mineral.

3.3. Geochronology results

All eight samples yielded two-point Sm-Nd ages whose uncertainties are reported at 2σ (Fig. 1 and Table 3). The high precision is attributed in large part to high ¹⁴⁷Sm/¹⁴⁴Nd ratios in the garnets. The ¹⁴⁷Sm/¹⁴⁴Nd ratios for the acid-cleansed garnet samples range from 1.5 to 3.8, with a mean of 2.4. The lone garnet sample that was not acid cleansed (Gurskøy) has a significantly lower ¹⁴⁷Sm/¹⁴⁴Nd ratio of 0.7.

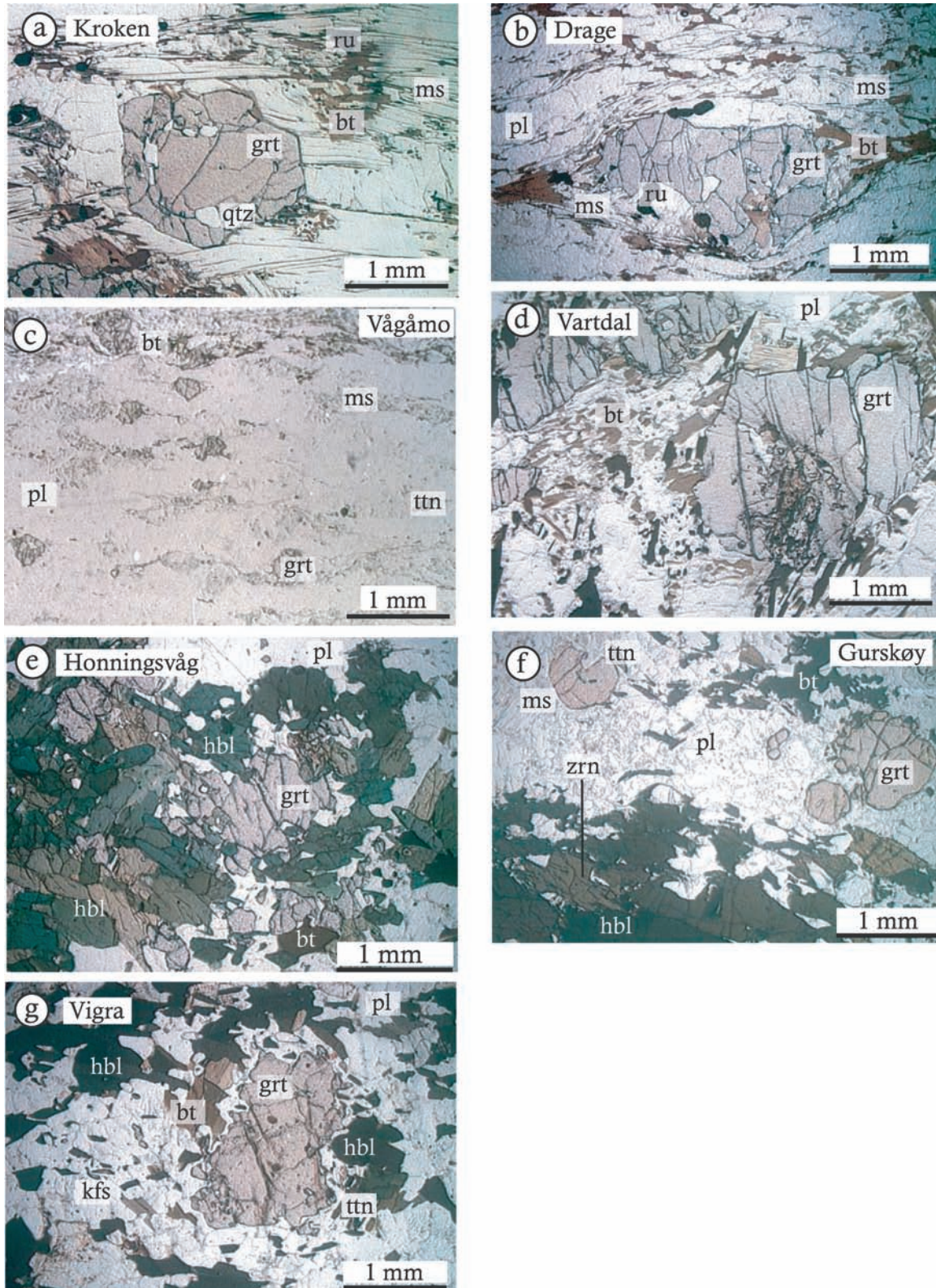


Fig. 3. Photomicrographs in plane-polarized light. a) Kroken; K-white mica (+ garnet) breaking down to biotite. b) Drage; biotite + plagioclase forming from K-white mica breakdown. c) Vågåmo; small garnets (<400 μm) in abundant quartz + plagioclase; minor K-white mica and titanite. d) Vartdal; biotite + plagioclase symplectite after garnet + K-white mica. e) Honningsvåg; garnet decomposing to biotite + hornblende + plagioclase. f) Gurskøy; rounded garnets with the largest breaking down to hornblende + plagioclase. g) Vigra; garnet (+ K-white mica ?) breaking down to biotite + plagioclase + hornblende. Mineral abbreviations after Kretz (1983); all K-white mica abbreviated as ms.

Table 3. Samarium–Neodymium isotopic data for gneisses from the Western Gneiss Region, Norway

Sample	Concentration (ppm)		$\frac{^{147}\text{Sm}}{^{144}\text{Nd}}$	$\frac{^{143}\text{Nd}}{^{144}\text{Nd}}$	Age ^a (Ma)	$\epsilon_{\text{Nd}(t)}$ ^b
	Sm	Nd				
Gurskøy (8815G6)						
Grt	2.30	1.99	0.702	0.513591 ± 5	410.3 ± 2.5	−7.9
Wr	12.37	63.58	0.118	0.512019 ± 7		
Vigra (P6817A2)						
Grt	2.18	0.85	1.546	0.515645 ± 11	406.9 ± 1.5	−11.5
Wr	9.82	52.74	0.113	0.511825 ± 8		
Kroken (rims) (P6805A2R)						
Grt	0.80	0.13	3.846	0.522017 ± 39	418.1 ± 1.6	−12.0
Wr	8.03	44.69	0.109	0.511783 ± 6		
Vartdal (P5627I5)						
Grt	3.33	0.83	2.424	0.518125 ± 7	398.5 ± 0.7	−6.3
Wr	5.59	30.92	0.109	0.512087 ± 6		
Vågåmo(P6808D2)						
Grt	0.97	0.33	1.759	0.522574 ± 11	921.7 ± 1.3	9.6
Wr	3.47	16.80	0.125	0.512695 ± 7		
Honningsvåg (P6806A3)						
Grt	0.28	0.12	1.471	0.516913 ± 38	587.3 ± 4.2	−12.3
Wr	11.07	75.05	0.089	0.511597 ± 7		
Drage (P6807G)						
Grt	3.78	1.05	2.172	0.517132 ± 8	403.9 ± 0.8	−14.2
Wr	3.53	17.02	0.125	0.511720 ± 6		
Kroken (cores) (P6805A2C)						
Grt	0.04	0.0070	3.264	0.520435 ± 21	417.3 ± 1.1	−11.4
Wr	8.03	44.69	0.109	0.511813 ± 7		

^a Ages are 2-point garnet–whole-rock isochrons.

^b $\epsilon_{\text{Nd}(t)}$ calculated using present-day ratios of $^{146}\text{Nd}/^{144}\text{Nd} = 0.7219$ and $^{143}\text{Nd}/^{144}\text{Nd} = 0.512638$ for CHUR; t is the age of the sample in Ma. Analysis by thermal ionization mass spectrometry at Boston University. $\lambda^{147}\text{Sm} = 6.54 \times 10^{-12} \text{ yr}^{-1}$. Errors in Nd isotope ratios are internal analytical 2 s.e. and refer to least-significant digits. Isochron ages calculated using *Isoplot* v. 3.09a (Ludwig, 2003). Age uncertainties were calculated using the poorer of the 2 sigma internal analytical precision for $^{143}\text{Nd}/^{144}\text{Nd}$ (reported above) or the within-barrel external precision (*i.e.* 0.000007 standard deviation for $^{143}\text{Nd}/^{144}\text{Nd}$). Uncertainty in $^{147}\text{Sm}/^{144}\text{Nd} = 0.1\%$ based on calibrations of the mixed Sm/Nd spike provided to the BU TIMS Facility by Prof. Donald DePaolo at UC Berkeley.

The oldest age, 921.7 ± 1.3 Ma (Vågåmo), came from the easternmost part of the Western Gneiss region, closest to the foreland (Fig. 1). Six of the samples from the UHP–HP core of the orogen yielded garnet ages from 418.1 ± 1.6 Ma to 398.5 ± 0.7 Ma; one, from Honningsvåg, is older, at 587.3 ± 4.2 Ma.

4. Geochemical modeling

Geochemical modeling of phase relations and mineral compositions provides insight into the P – T history of a rock: i) garnets preserving compositional zoning can be used to interpret pressures and temperatures of growth; ii) rutile can be used as a qualitative estimate of pressure; and iii) thermobarometry of equilibrated minerals can define equilibration conditions. This section first describes the major- and trace-element zoning within garnet. It then presents geochemical modeling results for the stability of garnet, rutile and K-white mica. Finally, thermobarometry of equilibrium phase assemblages are reported.

4.1. Garnet zoning

4.1.1. Major-element zoning

Forward modeling of major-element zoning in garnet can help estimate the pressures and temperatures at which a garnet grew. In the samples analyzed in this study, there are two compositional types of garnet. Garnets from Kroken, Vartdal, Vågåmo and Vigra are characterized by rimward-decreasing Mn and rimward-increasing Mg#, consistent with prograde growth (Fig. 4). Vigra and Vartdal also show sharp increases in Mn content at the rims. Honningsvåg, Gurskøy and Drage are compositionally homogenous except for large ($\sim 200\%$) increases in Mn and decreases in Mg# in the outer tens of micrometers. These rim features are typical of garnets that have undergone partial resorption (Kohn & Spear, 2000). The volume of garnet resorbed in the Vigra and Vartdal samples was calculated (Kohn & Spear, 2000) assuming spherical garnet and a linear decrease in Mn content of the resorbed portion. This approach implies that the Vigra garnets lost $\sim 65 \mu\text{m}$ (22 % of the garnet volume) during resorption and the Vartdal garnets lost $\sim 35 \mu\text{m}$ (5 vol%).

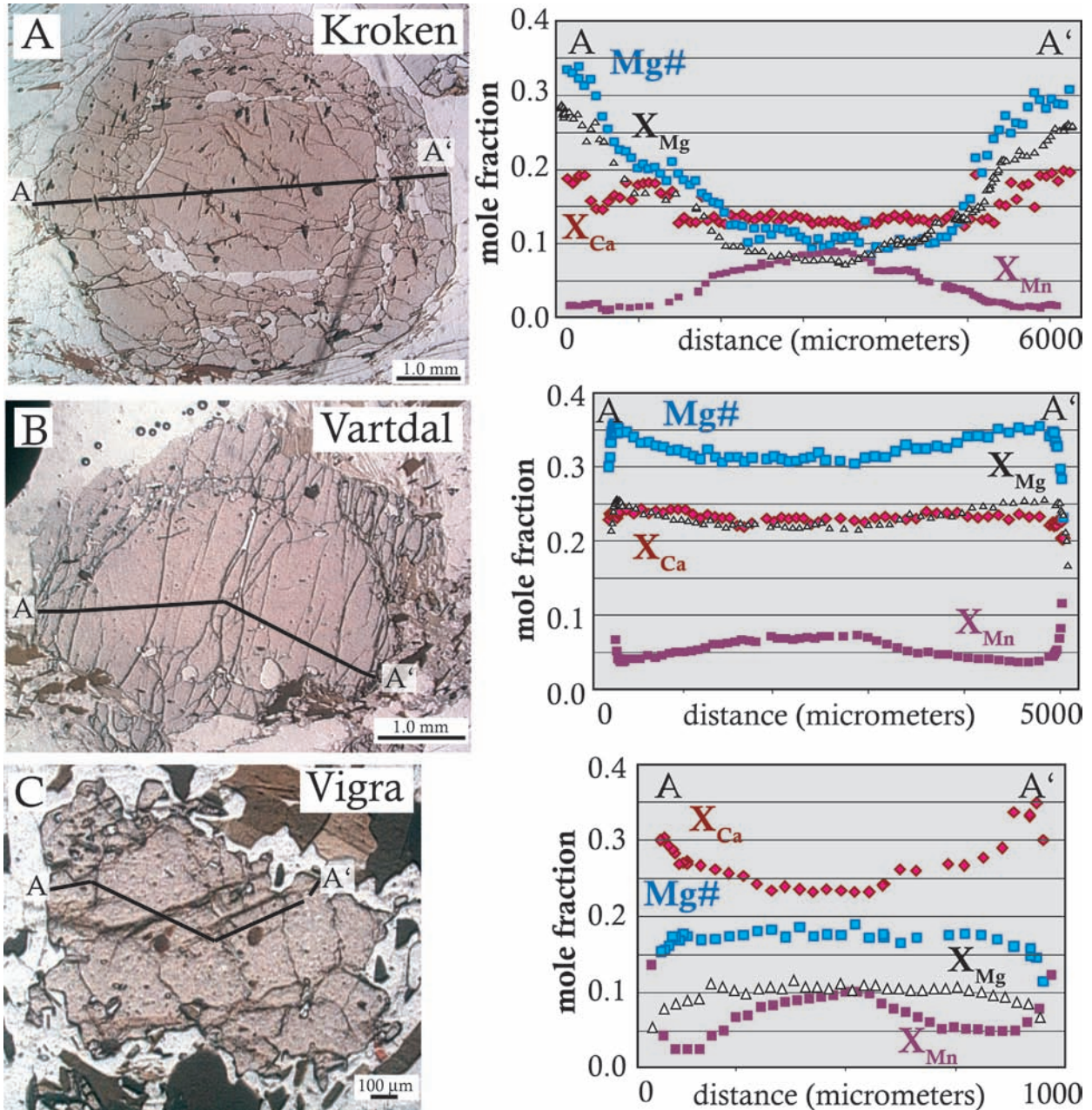


Fig. 4. Photomicrographs in plane-polarized light of garnets from A) Kroken, B) Vartdal and C) Vigra. Black lines mark electron microprobe traverses. Mole fraction of Ca and Mg# [$\text{Mg}/(\text{Mg}+\text{Fe})$] in garnet along these transects were correlated with *Perple_X* predicted garnet compositions to estimate the P - T of garnet growth (Figure 6). Mole fractions of Mn and Mg, also measured along the electron microprobe traverses, are plotted for comparison.

4.1.2. Trace-element zoning

Understanding the distribution of rare-earth elements in garnet is critical for interpreting Sm-Nd ages, in particular whether the age records primary growth or diffusional resetting during subsequent heating and cooling. Garnet preferentially incorporates heavy rare-earth elements, yielding, for example, growth zoning characterized by high Lu concentrations in the cores and steep decreases toward the rims (Lapen *et al.*, 2003; Skora *et al.*, 2006; Kylander-Clark *et al.*, 2007). Because rare-earth elements

diffuse through garnet at approximately the same rate (Carlson, 2005), Lu – the most-abundant HREE in garnet – can be used as a proxy for Sm and Nd zoning. If Lu zoning is preserved, it can be inferred that Sm and Nd have also not been significantly diffusively modified, in which case Sm-Nd ages will record primary growth. Moreover, REE diffusion in garnet is slower than major-element diffusion (Spear & Kohn, 1996; Tirone *et al.*, 2005; Dutch & Hand, 2009), such that rare-earth element zoning can be preserved during limited ($< \sim 10$ Myr)

exposure to high temperatures (*i.e.* $> \sim 700$ °C) even if major-element zoning is not. Therefore, garnet resorption should be characterized by a spike in Lu at the rims, just like Mn.

Trace-element zoning in garnet was measured via laser ablation on a Thermo Element 1 magnetic-sector ICP-MS at the University of California, Santa Cruz (Fig. 5). Garnets were continuously ablated using a New Wave 213 laser to produce rim–core–rim transects

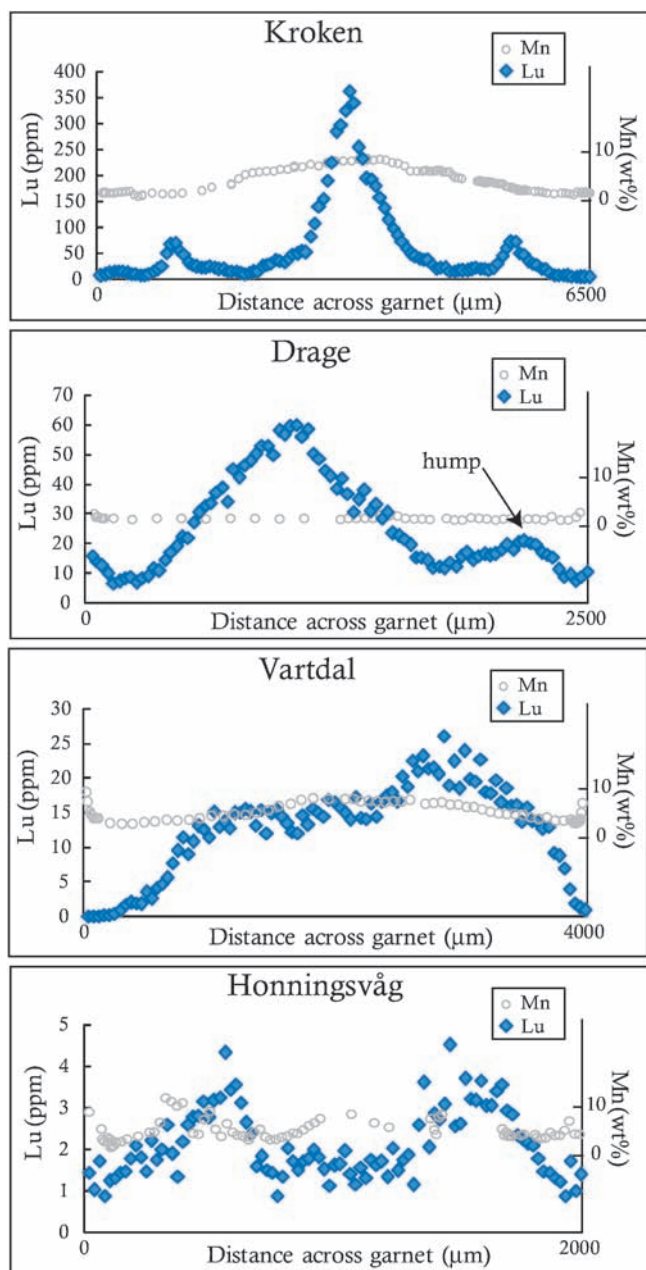


Fig. 5. Lu zoning (blue) from rim to core to rim in representative garnets from 4 samples. All four of these samples retain some form of Lu zoning. The HP gneisses–Kroken and Drage–have the highest concentrations of Lu, whereas Vartdal and Honningsvåg have from a factor of 2 to 2 orders of magnitude less Lu. See text for discussion of Lu hump in the Drage garnet. Mn zoning (gray) shown for comparison to major-element zoning.

across each grain. The time lag between laser and collector inherent in this style of sample collection produces smearing of the data. Each laser path in Fig. 5 proceeds from left to right; asymmetry as a result of residence time in the laser cell yields a tail on the right side of each peak. The abundance of ^{29}Si was used as an internal standard, and calibrated against electron microprobe measurements of Si for each garnet. The measured ratios were fractionation corrected using NIST 610 and 612 glasses.

Lu concentrations in the Kroken garnets are highest at the core and decrease rimward. These garnets also have humps approximately two-thirds the distance from the core to the rim. The Drage sample is similar, but the Lu hump is smoother and only located on one side. The increased Lu concentrations in the outermost 30 μm match Mn increases. The Vartdal garnets preserve high Lu concentrations in the cores, and concentrations decrease rimward. The Honningsvåg garnets have “M”-shaped Lu concentrations that are broadly consistent with the Mn zoning at the rims, but Mn and Lu zoning differ in the garnet core.

4.2. Geochemical modeling

Geochemical modeling was conducted with *Perple_X* (Connolly & Petri, 2002) and *Thermocalc* (Powell & Holland, 1988) using whole-rock compositions determined using ICP-MS at Washington State University (Table 1). As with all modeling of this type, uncertainties stem from the choice of activity models, the degree to which equilibrium was attained, and the influence of elements not measured or considered. The models nevertheless provide insight into the P – T conditions attained and recorded by minerals, and the effects of bulk composition on mineral reactions, compositions and modes. The H_2O content of the bulk composition is particularly important, but cannot be known for each rock at the time of reaction; accordingly, we explored the effects of varying the H_2O content from 0.1 to 5 wt%, emphasizing H_2O contents compatible with the hydrous mineral abundance of each sample (Table 1). Although the locations of reactions involving garnet vary with the abundance of H_2O , in all cases garnet is more stable at higher pressures and temperatures.

4.2.1. Garnet

To evaluate pressures and temperatures of garnet growth, forward models were calculated with *Perple_X* v. 6 and the 2002 Holland and Powell database. Activity models used in this study are listed in Appendix A (supplementary material freely available online at <http://eurjmin.geoscienceworld.org/>). Bulk-rock compositions were used to calculate equilibrium phase assemblages, mineral modes, and mineral compositions for each sample from 0.1 to 4.0 GPa, and 300 to 800°C. Mn was excluded from *Perple_X* because it stabilizes

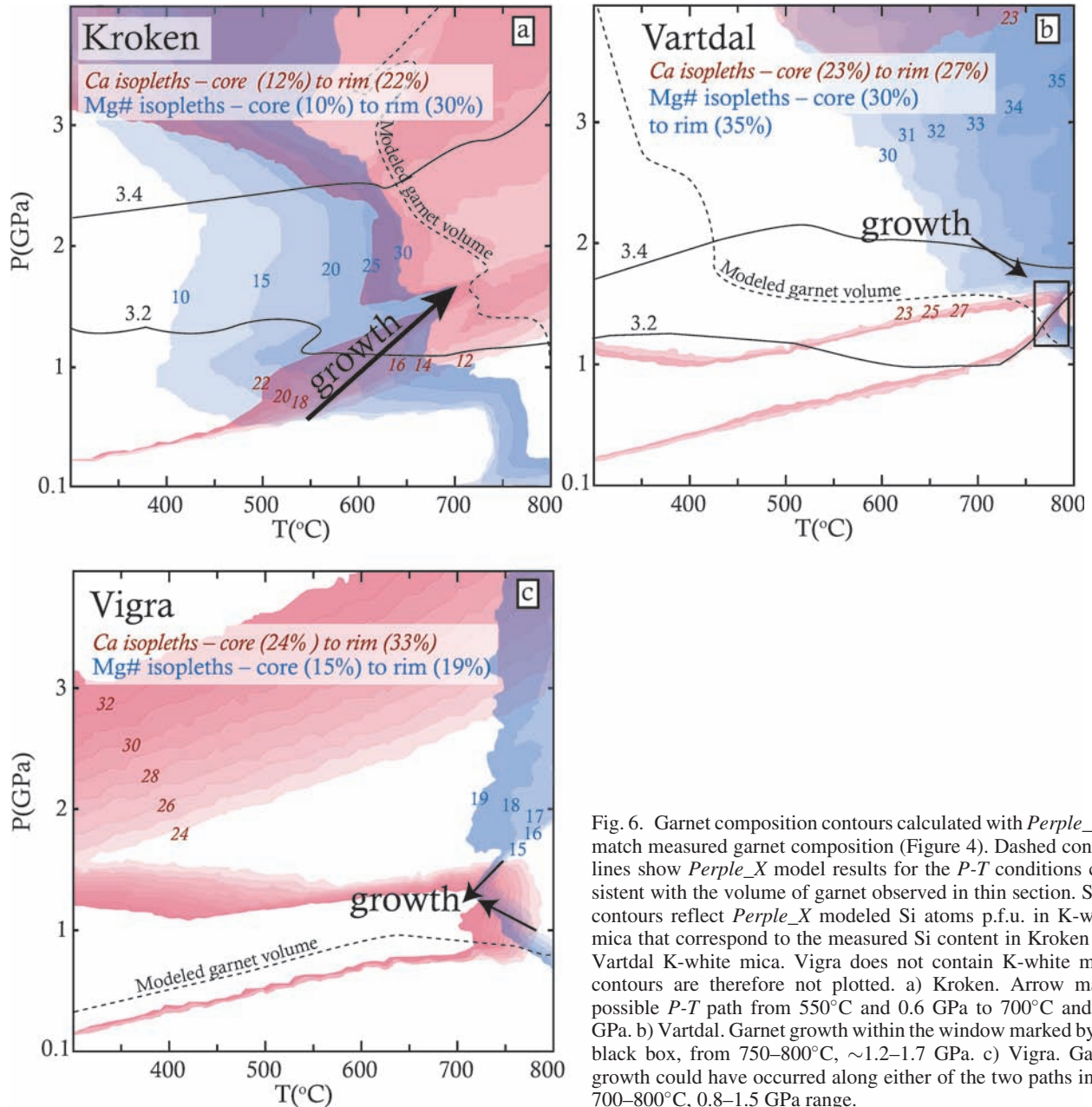


Fig. 6. Garnet composition contours calculated with *Perple_X* to match measured garnet composition (Figure 4). Dashed contour lines show *Perple_X* model results for the P - T conditions consistent with the volume of garnet observed in thin section. Solid contours reflect *Perple_X* modeled Si atoms p.f.u. in K-white mica that correspond to the measured Si content in Kroken and Vartdal K-white mica. Vigra does not contain K-white mica; contours are therefore not plotted. a) Kroken. Arrow marks possible P - T path from 550°C and 0.6 GPa to 700°C and 1.7 GPa. b) Vartdal. Garnet growth within the window marked by the black box, from 750–800°C, ~1.2–1.7 GPa. c) Vigra. Garnet growth could have occurred along either of the two paths in the 700–800°C, 0.8–1.5 GPa range.

garnet to unrealistically low temperature (Mahar *et al.*, 1997; Holler & Stowell, 2008). Electron microprobe measurements of Ca and Mg# zoning in garnet (Fig. 4) were then compared to these calculations to assess the range of pressures and temperatures over which garnet grew (Fig. 6). These comparisons suggest that the Kroken garnet grew during prograde metamorphism beginning at 550 °C and 1.0 GPa and ending at 700°C and 1.7 GPa. The Vartdal garnet grew at conditions of 750–800°C and 1.2–1.6 GPa, and the Vigra garnet around 700°C and 1.0–1.6 GPa (Fig. 6).

>The same methods were followed to determine equilibration conditions for the homogeneous garnets in the Vågåmo, Honningsvåg, Gurskøy and Drage samples

(Fig. 7). The data suggest re-equilibration of the Vågåmo sample at 1.0–0.7 GPa, 550–650 °C, Honningsvåg at ~1.0 GPa, 700–750 °C, Gurskøy at 1.3–0.9 GPa, 675–725 °C and Drage at 2.4–1.0 GPa, 575–700 °C.

4.2.2. Rutile

Rutile is a common accessory phase in the quartzofeldspathic rocks of the WGR. Because its stability depends chiefly on pressure and bulk composition, it can be used as a qualitative estimate of pressure. In the garnet-bearing samples analyzed in this study, rutile is included in garnet in the Kroken, Drage, Vartdal and Gurskøy samples and is a matrix mineral in the

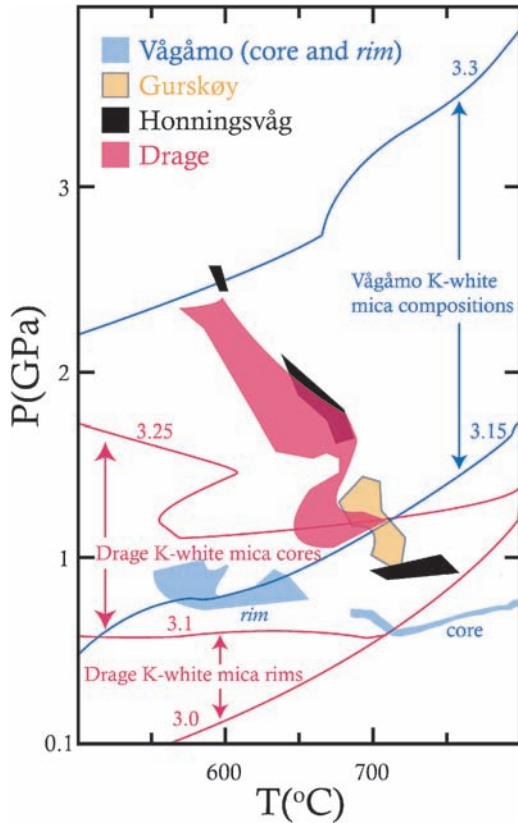


Fig. 7. Shaded domains represent the pressures and temperatures of garnet (re)equilibration. Garnet rim compositions for the Vågåmo sample are different from the core and therefore are plotted as two distinct polygons. Blue contours are the modeled Si atoms p.f.u. in measured K-white mica for the Vågåmo sample. The distinct P - T stability fields for core and rim K-white mica in the Drage sample are plotted in pink. Honningsvåg and Gurskøy do not contain K-white mica.

Vågåmo sample. Phase diagrams constructed with *Perple_X* show that rutile is stable above 0.6 GPa in the Vartdal, Kroken, Drage and Honningsvåg samples, above 1.2 GPa in the Vigra sample, and above 1.5 GPa in the Gurskøy and Vågåmo samples (Figure in

Appendix B, supplementary material freely available online at <http://eurjmin.geoscienceworld.org/>).

4.2.3. K-white mica

The number of Si atoms per formula unit (p.f.u.) in K-white mica depends on bulk composition and pressure, as shown in Figs 6 and 7 as calculated by *Perple_X*. These isopleths were compared to the compositions of K-white mica measured by electron probe (data in Section 3.2). The Si content of the Kroken K-white micas suggests a stability field between 1.2 and 3.2 GPa (Fig. 6), the Vartdal K-white mica from ~ 1.0 to 2.1 GPa (Fig. 6). The Drage K-white mica cores suggest higher pressures (0.6 to 1.7 GPa) than the rims (0.1 to 0.6 at T below 700°C; Fig. 7), and the Vågåmo K-white micas were apparently stable between 0.8 and 3.8 GPa at 600–800°C (Fig. 7).

4.2.4. Thermobarometry

The P - T conditions of metamorphism were calculated with *Thermocalc* (Powell & Holland, 1988) for samples with coarse-grained phases interpreted to be in equilibrium. Table 4 lists the reactions used, and Table 5 lists the mineral compositions used. Three samples indicate recrystallization at temperatures of 700–800 °C and 0.8–1.1 GPa. Thermometry of the far-east sample, Vågåmo, suggests equilibration at lower temperature for an assumed P of 1.1 ± 0.2 GPa.

5. Interpretation

This study was prompted by two fundamental questions about the timing and significance of phase transformations in quartzofeldspathic gneisses during subduction and exhumation. This section presents the interpreted histories for quartzofeldspathic gneisses based on the data presented above. The broader-scale implications of these histories are discussed in Section 6.

Table 4. *Thermocalc* reactions and P - T estimates.

	Reactions used with <i>Thermocalc</i>	Pressure (GPa)	Temperature (°C)
Vågåmo (P6808D2)	py + ann = alm + phl	$1.1 \pm 0.2^*$	560 ± 100
		* assumed P	
Vigra (P6817A2)	2py + 4gr + 3ts + 12q = 12an + 3tr 4gr + 5alm + 3ts + 12q = 3py + 12an + 3fact 5py + 3fact = 5alm + 3tr	0.8 ± 0.2	700 ± 100
Drage (P6807G)	py + gr + mu = 3an + phl gr + alm + mu = 3an + ann py + ann = alm + phl	1.1 ± 0.2	725 ± 50
Honningsvåg (P6806A3)	2py + 4gr + 3ts + 12q = 12an + 3tr 5py + 3fact = 5alm + 3tr	0.9 ± 0.2	725 ± 65

Table 5. Mineral compositions used with *Thermocalc*. Abbreviations after Kretz (1983).

	SiO ₂	Al ₂ O ₃	TiO ₂	FeO ^a	Cr ₂ O ₃	MnO	MgO	CaO	Na ₂ O	K ₂ O
<i>Vågåmo (P6808D2)</i>										
grt 323	37.3	20.2	<	30.2	<	8.0	1.0	2.8	0.1	<
pl 191	68.3	20.0	<	<	<	<	<	0.6	11.6	0.1
bt 399	36.1	16.9	2.0	25.0	<	0.4	5.5	<	0.1	9.8
ms 293	45.7	29.2	0.2	4.8	<	0.1	1.3	<	0.3	10.7
<i>Vigra (P6817A2)</i>										
grt 58	38.0	20.0	0.1	26.0	<	3.2	3.0	10.0	<	<
pl 157	57.1	27.0	<	0.4	<	0.1	<	9.2	6.9	0.1
bt 137	38.8	13.5	1.5	21.2	<	0.6	6.8	11.4	1.1	2.0
hbl 205	40.3	13.7	1.5	19.4	<	0.5	7.1	11.2	1.0	2.0
<i>Drage (P6807G)</i>										
grt 33	38.0	21.6	<	28.3	<	0.9	4.6	6.9	<	<
pl 146	60.6	24.4	<	0.1	<	<	<	5.8	8.2	0.1
bt 72	35.4	18.1	1.6	19.7	<	0.2	10.3	<	0.1	9.5
vms 396	47.5	30.2	0.6	2.3	0.1	0.1	0.7	0.1	0.5	8.9
<i>Honningsvåg (P6806A3)</i>										
grt 25	38.9	21.8	<	27.1	<	1.0	5.1	7.8	<	<
pl 262	62.2	24.0	<	<	<	<	<	5.7	8.5	0.1
bt 22	37.4	18.6	2.1	16.9	<	0.3	10.8	0.2	0.1	9.4
hbl 463	40.3	16.0	0.4	18.2	<	0.5	7.8	11.1	1.5	0.7

Mineral abbreviations after Kretz (1983); '<': below electron microprobe detection limit. ^aAll Fe treated as FeO.

5.1. Garnet-bearing quartzofeldspathic gneisses

The 921.7 ± 1.3 Ma garnet age for the easternmost gneiss sample – Vågåmo (*Vå*) – is equivalent to the ~ 930 – 900 Ma Proterozoic granulite-facies event recognized elsewhere in the WGR (Cohen *et al.*, 1988; Root *et al.*, 2005; Bingen *et al.*, 2008). Garnet in this rock is homogeneous, precluding recovery of the *P*–*T* path; Fe–Mg exchange thermometry between garnet and biotite indicates recrystallization temperatures of 560 ± 100 °C for assumed pressures of 1.1 ± 0.2 GPa, but the absence of garnet zoning implies that this is colder than the peak temperature. Matrix rutile suggests that this sample equilibrated at pressures greater than 1.2 GPa. The presence of zoisite spicules in the plagioclase grains suggests that the rock might have undergone incipient eclogite-facies metamorphism. Titanite ages in this region are Precambrian (Kylander-Clark *et al.*, 2008), whereas ⁴⁰Ar/³⁹Ar ages for K-white micas are Scandian, implying that Scandian temperatures were in the 400–600 °C range. This sample is interpreted to represent the portion of the WGR that did not recrystallize at high pressure and did not grow new garnet during the Scandian; its history is shown schematically in Fig. 8A.

The age of the Honningsvåg (*H*) sample – 587.3 ± 4.2 Ma – is interpreted to be either a mixture of Proterozoic and Caledonian garnet growth or re-equilibration. Although the garnet is largely homogeneous in major element concentrations (some Mn zoning exists), the Lu zoning suggests two distinct periods of garnet growth (Fig. 5). The preservation of Lu zoning implies that the Sm and Nd isotopes were not completely homogenized. The age could therefore represent either partial resetting of Proterozoic garnet or a mixture of Proterozoic and Caledonian garnet growth.

The calculated 725 ± 65 °C, 0.8 ± 0.2 GPa equilibration condition (Table 4) is consistent with either growth or re-equilibration. Because new growth and re-equilibration are equally plausible and the age is mixed, the garnet growth history, and thus the phase transformation history, are ambiguous.

The Kroken (*K*) sample is interpreted to have undergone prograde garnet growth at HP for two reasons: the core and rim ages – 417.3 ± 1.1 Ma and 418.1 ± 1.6 Ma, respectively – are equivalent to the 419.5 ± 4.3 Ma Sm–Nd age of the nearby Verpeneset UHP eclogite (Kylander-Clark *et al.*, 2007), and *Perple_X* modeling of the garnet composition suggests prograde growth up to 700 °C and 1.7 GPa. *Perple_X* modeling further suggests that most garnet growth occurred at pressures <1.4 GPa, and that the modal abundance of garnet could have increased by only a few percent above 1.7 GPa (Fig. 10B). This small amount of predicted garnet growth at >1.7 GPa may explain why garnet preserving compositions compatible with UHP growth is so rare in quartzofeldspathic gneisses. Furthermore, the rims show no evidence of resorption, suggesting that the entire history of garnet growth was preserved. Rutile inclusions in garnet require growth at pressures greater than 0.5 GPa, which is consistent with the modeled garnet growth history. This sample reflects the garnet growth history shown in Fig. 8B and represents the end-member model shown in Fig. 2B.

The preservation of both major-element and Lu zoning in the Vartdal (*Va*) garnets (Fig. 4 and 5) suggests that the 398.5 ± 0.7 Ma Sm–Nd age of this sample has not been diffusionally modified. *Perple_X* modeling of the garnet zoning implies growth over a narrow range of conditions at 750–800 °C and 1.5–1.7 GPa (Fig. 6). Garnet growth at

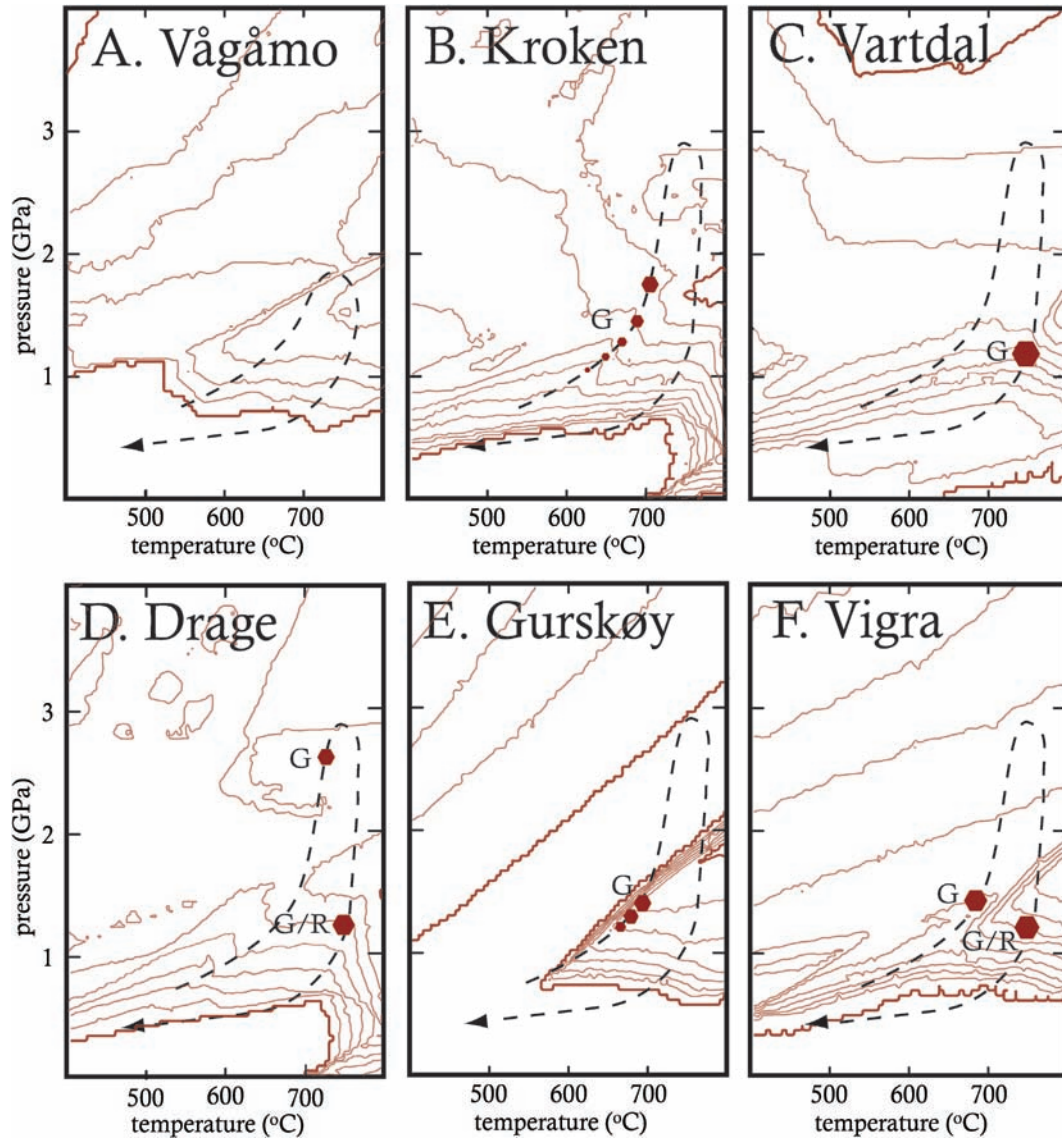


Fig. 8. Interpreted garnet growth histories and P - T paths for Kroken, Drage, Vågåmo, Gurskøy, Vartdal and Vigra samples. Red contour lines indicate modal garnet in each sample (2 % for each contour). Symbols indicate where garnet either grew (G) or re-equilibrated (R). Honningsvåg not shown because the sample does not retain any information about the garnet growth history or the P - T path.

higher pressures is unlikely to have occurred because the rock lacks pyrope–grossular garnet (*Perple_X* calculations for 700°C and 3.5 GPa predict $\text{prp}_{26}\text{alm}_{52}\text{grs}_{22}$) and phengitic mica with >3.4 Si atoms p.f.u. (Fig. 6). Instead, the inferred garnet growth conditions, the modal abundance of garnet in the sample, the young age of the garnet and the low Si content of the K-white mica are all consistent with garnet growth during exhumation (shown schematically in Fig. 2D). The textural relations between the garnet and the coarse-grained biotite suggest that they grew together with K-white mica. The symplectite of higher-titanium biotite and plagioclase post-dates the garnet-forming event, and likely occurred at pressures of 1.0–0.5 GPa and ~ 700 °C. The symplectite in this sample may represent a glimpse of the retrograde amphibolite-facies overprint that is characteristic of the western two-thirds of the region – in this

case, the preservation of symplectite shows the arrested retrograde reaction. Importantly, this sample shows no evidence of prograde metamorphic phase transformation, suggesting that the rock was metastable throughout subduction to HP. The garnets in this sample are interpreted to represent the growth history shown in Fig. 8C.

The polycrystalline quartz (PCQ) inclusion in one of the Drage (D) garnets suggests that these garnets originally formed at UHP conditions. Compositions from the rim of the garnet and matrix minerals yield pressures of 1.1 ± 0.2 GPa and temperatures of 725 ± 50 °C. The stark difference in pressure estimates between core (PCQ) and rim (thermobarometry) can be correlated to the ‘hump’ in Lu near the rim (Fig. 5), which suggests two garnet growth events. The Si contents of K-white mica also define two P - T stability fields (Fig. 7). Because the pressures inferred for the rim

are far below coesite stability, the rim likely represents additional garnet growth or re-equilibration with the matrix at garnet-amphibolite facies conditions. Like Kroken and Vartdal, the Drage garnet retains Lu zoning, which suggests that the Sm and Nd have not been completely homogenized. Therefore, the 403.9 ± 0.8 Ma age of this sample presumably represents a mix of UHP and amphibolite-facies growth, or partial resetting of the Sm-Nd age at amphibolite facies. These data are consistent with the growth history depicted in Fig. 2C, but could also represent a combination of Fig. 2C and 2D; these histories are shown in Fig. 8D.

The mm-scale garnets in the Gurskøy (*G*) sample are homogeneous in major elements except for a sharp increase in Mn at the rims. The composition of the garnet is consistent with growth at pressures of 1.0–1.5 GPa and 700 ± 25 °C (Fig. 7) and rutile inclusions in garnet also indicate garnet growth at >1.2 GPa (Appendix B). The lack of compositional zoning suggests either rapid growth or wholesale diffusional homogenization. The sharp increase in modal abundance of garnet in this *P-T* range (Fig. 8E) suggests rapid garnet growth, and may explain the absence of zoning. The Sm-Nd age of 410.3 ± 2.5 Ma agrees with ages from a nearby eclogite of 412.0 ± 4.7 Ma (Lu-Hf) (Kylander-Clark *et al.*, 2007) and suggest that the age reflects prograde garnet growth during subduction (*e.g.* Fig. 2B). The presence of coarse-grained idioblastic amphibole and titanite also suggest growth at garnet-amphibolite-facies conditions. Importantly, after growing garnet, this rock behaved metastably for the remainder of subduction and exhumation. The garnet growth history is represented by Fig. 8E.

The Vigra (*Vi*) garnets preserve major-element zoning in Mn and Ca, but Fe and Mg are homogeneous, suggesting a narrow *P-T* range during growth (or re-equilibration). The age of this sample (406.9 ± 1.5 Ma) is equivalent to the Sm-Nd age of a nearby HP eclogite (402.7 ± 4.6 ; Kylander-Clark *et al.*, 2007), suggesting growth during subduction (Fig. 2B). However, *Perple_X* modeling indicates garnet growth at 700–750 °C and 1.0–1.6 GPa. Thermobarometry using garnet rims, matrix amphibole and plagioclase suggests (re-)equilibration at equivalent conditions of 700 ± 100 °C and 1.0 ± 0.2 GPa. These data are consistent with either new garnet growth or wholesale homogenization of prograde garnets during exhumation (Fig. 2D). The sample contains no rutile, but abundant titanite and matrix plagioclase, which indicate growth at pressures below 1.5 GPa. The data are all consistent with exhumation related growth – there is no evidence of prograde growth other than the agreement in age with a nearby eclogite. Although garnet growth during exhumation is favored, prograde growth cannot be conclusively ruled out. Therefore, both possible growth histories are illustrated in Fig. 8F.

In summary, the Vågåmo garnets grew during Proterozoic metamorphism, the Honningsvåg garnets during Proterozoic and Caledonian metamorphism, and the Kroken garnets during HP metamorphism. The Drage and Gurskøy garnets reflect a mix of prograde and post-(U)HP growth or partial diffusional re-equilibration; the *P-T* conditions of garnet growth cannot be established for these

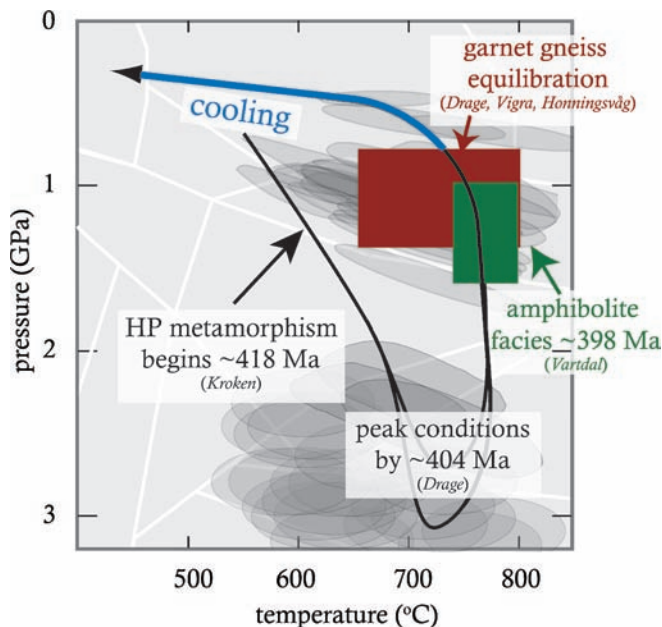


Fig. 9. Pressure–temperature–time path for the Western Gneiss Region, Norway (after Kylander-Clark *et al.*, 2007). Gray ellipses show previous *P-T* determinations for lithologies in the WGR. HP metamorphism, peak conditions and amphibolite-facies ages from Sm-Nd garnet–whole-rock isochrons (Table 3 and Figures 6 & 7) and garnet-bearing gneiss equilibration based upon *Thermocalc* estimates (Table 4).

samples because the garnet zoning has not been preserved. The Vartdal garnets (and possibly the Vigra garnets) grew during the post-UHP amphibolite-facies event.

5.2. *P-T-t* path of the Western Gneiss Complex

The data for all samples can be collectively used to further constrain the *P-T-t* path of the Western Gneiss Complex (Fig. 9). The Vågåmo sample demonstrates that the eastern WGC did not transform to high-pressure minerals during the Caledonian – rocks in the east record a maximum pressure of ~1.5 GPa. The Kroken sample represents prograde metamorphism during subduction (~418 Ma, 1.7 GPa, 700 °C). The Drage sample represents peak UHP conditions in the coesite stability field by 404 Ma. This is a minimum age for peak UHP metamorphism because this is likely a mixed age; UHP metamorphism could have ended earlier. The Vartdal sample represents post-UHP garnet-amphibolite-facies metamorphism (398 Ma, ~750–800 °C, 1.5–1.7 GPa). Final re-equilibration of the garnet-bearing gneisses occurred at 650–800 °C and 0.8–1.5 GPa (Vigra, Gurskøy and Honningsvåg). These data are broadly consistent with 420–400 Ma Lu-Hf and Sm-Nd ages for (U)HP eclogites (see summary in Kylander-Clark *et al.*, 2007) and 398–389 Ma titanite ages for the amphibolite-facies overprint (Kylander-Clark *et al.*, 2008), but also suggest decompression-induced garnet growth from 410 to 404 Ma.

6. Discussion

6.1. To what extent did the crust transform to (U)HP minerals?

One of the motivating questions in this study was a determination of the proportion of the crust that transformed to (U)HP minerals during subduction. The degree to which WGR continental rocks transformed to (U)HP minerals and then back to low-pressure minerals bears directly on issues such as the i) rheology of continental crust at high temperature and pressure (*e.g.*, whether transformational plasticity strongly influences rheology), ii) gravitational body forces during subduction and exhumation, and iii) the mechanisms by which UHP rocks are exhumed.

To estimate the amount of crust that transformed in the subducted and exhumed WGR continental crust, we revisit the lithologies from Section 2.3; paragraph numbers are keyed to Fig. 10. The histories of the garnet-bearing quartzofeldspathic rocks – roughly 30 % of the WGR – are interpreted as follows:

- (1) *Gneiss with subduction-related garnet (e.g., Kroken, Gurskøy)*. Compositional zoning suggests that the Kroken and Gurskøy garnets grew during subduction, implying that these

gneisses transformed along the prograde path to UHP. Portions of the gneiss back-reacted during exhumation to form the current assemblage: garnet + K-white mica + biotite + plagioclase + quartz ± hornblende. Other WGR garnet-bearing gneisses may also have transformed at UHP, but individual garnets may not preserve evidence of growth at UHP because only a few volume percent of garnet is predicted to grow in such bulk compositions at pressures >1.5 GPa.

- (2) *Gneiss with (U)HP garnet modified or overgrown by amphibolite-facies garnet (e.g., Drage)*. A polycrystalline quartz inclusion in one of the Drage garnets suggests growth at UHP. Zoning suggests either mantling by secondary garnet during garnet-amphibolite-facies overprinting or diffusional modification of major elements. These data suggest that some gneisses may contain garnet grown at UHP that was diffusively modified and/or mantled by garnet grown during exhumation.
- (3) *Gneiss with amphibolite-facies garnet (e.g., Vartdal, Vigra)*. Major-element zoning suggests garnet growth at ~750–800 °C and 1.5 ± 0.3 GPa. The best explanation for these rocks is Fig. 2D, which depicts *no phase*

pre-eclogite facies	eclogite facies	amphibolite facies
≤ 85% WGC quartzofeldspathic gneiss (including 10% biotite granitic and 5% two-mica tonalitic gneisses)	→ 1-5% eclogite-facies gneiss → 10-15% garnet-amphibolite-facies gneiss → 65-70% metastable gneiss	→ 1% eclogite-facies gneiss [2?] → 25-34% garnet-amphibolite-facies gneiss ± melt [1-3] → 50-60% untransformed, metastable gneiss [4 and all garnet-free gneiss]
≥ 5% biotite gneiss	5% biotite gneiss	5% biotite gneiss [5]
1% quartzite	1% quartzite/coesitite	1% quartzite [6]
≥ 5% kfs augen gneiss	5% kfs augen gneiss	5% kfs augen gneiss [7]
≥ 1% granulite	1% granulite	1% granulite [8]
2% basalt/gabbro	→ 0.2% basalt/gabbro → 1.8% eclogite	→ 0.2% basalt/gabbro [9] → 0.9% eclogite [9] → 0.9% amphibolite [9]

Fig. 10. The transformation history of the Western Gneiss Region. Most mafic rocks transformed to eclogite; about half of those then retrogressed to amphibolite. Granulite, biotite gneiss and K-feldspar augen gneiss did not transform during subduction or exhumation. Quartzite presumably transformed to coesitite during subduction. A maximum of 5 % of the quartzofeldspathic gneiss transformed to eclogite facies, only ~1 % of which was preserved (not observed in this study). 10–15 % of the gneiss transformed at garnet-amphibolite facies during subduction. Most of the gneiss (65–70 %) did not transform at eclogite-facies, but another 10–19 % grew garnet during decompression. 50–60 % of the gneiss never transformed. Biotite gneiss, K-feldspar augen gneiss and granulite-facies gneiss constitute ~11 % of the WGR, but there may have been more of these bulk compositions that did transform during subduction and/or exhumation. Colors are intended as a visual guide to density. Numbers in square brackets refer to the discussion in Section 6.1 of the text.

transformations during subduction, but wholesale transformation, highlighted by garnet growth, during exhumation.

- (4) *Gneiss with Proterozoic garnet* (e.g., *Vågåmo*). No high-pressure phase transformation – other than the growth of minor zoisite – is evident in these gneisses.
The histories of the other five rock types from Section 2.3 remain as originally inferred:
- (5) *Biotite gneiss*. Seams of biotite gneiss constitute ~5 % of the WGR; they did not transform because they were stable at UHP conditions.
- (6) *Quartzite/coesite*. Quartzite layers constitute ~1 % of the WGR; whether these layers transformed to coesite and back to quartz has not been assessed.
- (7) *K-feldspar augen gneiss*. Centimeter-scale K-feldspar augen gneiss comprises ~5 % of the WGR. The coarse grain size, and the absence of jadeitic clinopyroxene, K-white mica and symplectite imply that these rocks did not transform at (U)HP. Any rocks of this bulk composition that were converted to high-pressure phases during subduction and then converted back into typical quartzofeldspathic gneiss during exhumation now fall in rock types 2 or 5.
- (8) *Granulite-facies orthogneiss*. Approximately 1 % of the WGR is composed of relict Precambrian granulite-facies rocks that did not transform to eclogite-facies minerals (Wain *et al.*, 2001). Again, a larger, unknown fraction of granulite-facies rocks may have been converted into gneiss type 2 or 5.
- (9) *Mafic bodies*. Comprising ~2 vol% of the WGR, roughly 90 % of the mafic bodies transformed to eclogite, and about half of those back-reacted during exhumation to amphibolite-facies assemblages.

The compositions in these two categories – non-WGC lithologies and garnet-bearing WGC – represent less than half of the rocks in the WGR (~15 and 30 %, respectively). The remainder of the WGR is composed of plagioclase-bearing quartzofeldspathic gneisses that contain no evidence of high-pressure metamorphism. Although there are no data that bear directly on these garnet-free quartzofeldspathic gneisses, the data presented in this study suggest that even garnet-bearing lithologies show evidence of metastability through eclogite-facies conditions. For example, the Vigra and Vartdal samples show no evidence of garnet growth during subduction, but indicate decompression garnet growth associated with exhumation. Only two samples indicate prograde garnet growth – Kroken and Gurskøy – and neither suggests growth at pressures >2 GPa. The only garnet-bearing sample that may have transformed at UHP – Drage – does not retain any evidence in the compositional zoning to suggest that garnet formed at UHP.

Why did the Kroken and Gurskøy samples transform during subduction while the other samples remained metastable? The Kroken sample comes from within a UHP domain whereas the Gurskøy sample does not, so

differences in peak pressure cannot explain the transformation behavior. They contain different mineralogy – amphibole and titanite in Gurskøy, K-white mica in Kroken – suggesting that protolith mineralogy may have played a role. Although both samples are compositionally similar to the other five samples, they have the highest Al₂O₃/SiO₂ ratio (0.34 and 0.28 respectively, compared with 0.21 to 0.24 for the other 5 samples; data from Table 1), which could also have played a role.

These data inform the transformation history of garnet-free gneisses. First, even some garnet-bearing quartzofeldspathic gneisses do not record UHP mineral compositions or assemblages. Instead, the garnet reflects growth at garnet-amphibolite facies. If none of the garnet-bearing gneisses indicate garnet growth at UHP, it is unlikely that garnet-free gneisses transformed to eclogite-facies minerals and then underwent wholesale retrogression to erase all history of that metamorphism. Second, bulk composition affects the timing and extent of mineral transformation – our models shows garnet growth below 2 GPa – and minor differences in composition may control whether growth occurs along the prograde or retrograde path. Further study of a wider variety of bulk compositions and *PT* conditions – including the central portion of the (U)HP terrane – will reveal how robust these interpretations are. These findings suggest that metastability and disequilibrium were the rule, not the exception, in quartzofeldspathic gneisses of the WGR.

In summary, 65–70 % of the WGR gneiss may have been metastable during subduction. The only compositions that must have transformed are the eclogite and the eclogite-facies gneiss (estimated at 1–5 % from other studies; not seen in this study). Some fraction of the gneiss transformed during subduction at garnet-amphibolite facies conditions (~10–15 %) and another fraction (~10–19 % more) transformed during exhumation at garnet-amphibolite facies conditions. In total, ~2/3 of the WGR may never have transformed – these lithologies include quartzofeldspathic gneiss, biotite gneiss, K-feldspar augen gneiss, granulite and some basalt/gabbro bodies. At UHP, perhaps less than 8 % of the WGR was in equilibrium at eclogite-facies; 92 % was metastable.

6.2. Geodynamic implications

The data presented in this paper require that the bulk of the quartzofeldspathic rocks of the WGR (Fig. 10) did not recrystallize to (U)HP minerals during subduction – in spite of temperatures > 700 °C and pressures > 2 GPa. This interpretation diverges with earlier studies. For example, Krabbendam *et al.* (2000) concluded that local bodies were metastable, but that the bulk of the gneiss transformed at (U)HP. Additionally, our interpretation of garnet growth during *exhumation* contrasts with previous studies. The delayed phase transformations in these rocks may be attributed to fluid influx during decompression and exhumation (Straume & Austrheim, 1999; Engvik *et al.*, 2000).

Delayed phase transformations during the vertical motions of large-scale terranes have important implications for orogenesis. As noted by others (*e.g.* Dewey *et al.*, 1993; Austrheim *et al.*, 1997), reactions involving large changes in density can strongly influence aspects of orogenesis, including topography, material flow, and crustal thickness. Assume for the sake of simple illustration, that the WGR lithosphere was 100 km thick and that the upper-mantle portion was harzburgite with an average temperature of 1000 °C and immersed in 1300 °C asthenosphere of the same composition. The density difference between the mantle lithosphere ($\sim 3.34 \text{ g/cm}^3$; calculated following Hacker & Abers (2004)) and the asthenosphere ($\sim 3.31 \text{ g/cm}^3$) at these temperatures is only 0.03 g/cm^3 . If the WGR density remained at 2.8 g/cm^3 during subduction, a 100-km thick lithosphere would be positively buoyant only if the crust were $< 6 \text{ km}$ thick (Fig. 11). In contrast, if the WGR transformed to UHP minerals during subduction, it would have had an aggregate density of $\sim 3.2 \text{ g/cm}^3$ (a density increase of $\sim 14 \%$), and the WGR crust could have been as much as 20 km thick in a 100 km-thick lithosphere that was still negatively buoyant. Instead, our data suggest that the WGR could have remained at a density of 2.8 g/cm^3 throughout subduction until the pressure decreased to $\sim 1.0\text{--}1.6 \text{ GPa}$, at which point the quartzofeldspathic rocks of the WGR transformed to a higher density assemblage (3.0 g/cm^3) including garnet + K-white mica.

Our data also bear on the rheology of quartzofeldspathic crust at high pressure and temperature. Inferences of mid–lower crustal flow (Enkelmann *et al.*, 2006) have been taken to indicate that quartzofeldspathic rocks flow at

temperatures of 700–800 °C. In contrast, other studies (Lenze & Stöckhert, 2007) demonstrate that quartzofeldspathic rocks can be subjected to such temperatures and high pressures and remained undeformed. If the gneisses investigated in this study had been deformed and/or been exposed to catalyzing fluids at (U)HP, they would likely have transformed to (U)HP minerals (Koons *et al.*, 1987; Austrheim, 1998; Terry & Heidelbach, 2006); that they did not transform indicates that they did not deform.

Transformational weakening is often assigned a major role in crustal rheology because of the probability that fine-grained neoblasts will induce a switch to grain size-sensitive creep and higher strain rates. Our observations indicate that minimal phase transformations (and therefore minimal transformational weakening) occurred during subduction. Geodynamic models of crustal deformation – including subduction – should consider these implications.

7. Conclusions

Sm-Nd ages, mineral compositions and textures indicate that quartzofeldspathic gneisses in the Western Gneiss Region underwent five different phase-transformation histories. (1) The Vågåmo sample shows that the eastern WGR did not undergo wholesale recrystallization during subduction. (2) The Kroken and Gurskøy samples demonstrate that some rocks transformed during subduction. (3) The Drage sample shows that other rocks grew (ultra)high-pressure minerals (coesite) during subduction and then underwent significant overprinting, including garnet growth, during exhumation. (4) The mixed age and compositional zoning in the Honningsvåg sample indicates that Precambrian garnet locally persisted through subduction and subsequent garnet growth. (5) The Vardal and Vigra samples indicate metastability during subduction and garnet growth during exhumation.

These data collectively suggest that $\sim 1/3$ of the Western Gneiss Region transformed during prograde metamorphism at garnet-amphibolite facies, but only $\sim 8 \%$ continued transforming through eclogite facies. During exhumation, an additional $\sim 10\text{--}20 \%$ transformed at garnet-amphibolite facies conditions. More than 50 % of the Western Gneiss Region probably never transformed, suggesting widespread metastability of quartzofeldspathic rocks.

Acknowledgements: Funded by NSF EAR-0510453 to BRH. Geochronology was conducted in the Boston University TIMS Facility, funded by NSF MRI Grant EAR-0521266 and NSF Grant EAR-0547999 to EFB. J. Harvey assisted with TIMS analysis and sample preparation, and D. DePaolo provided the mixed $^{147}\text{Sm}/^{150}\text{Nd}$ spike used in this work. J. Hourigan and R. Franks assisted with TE analysis in garnet and G. Seward with EPMA and SEM analyses. H. Austrheim and W. Carlson provided thoughtful reviews.

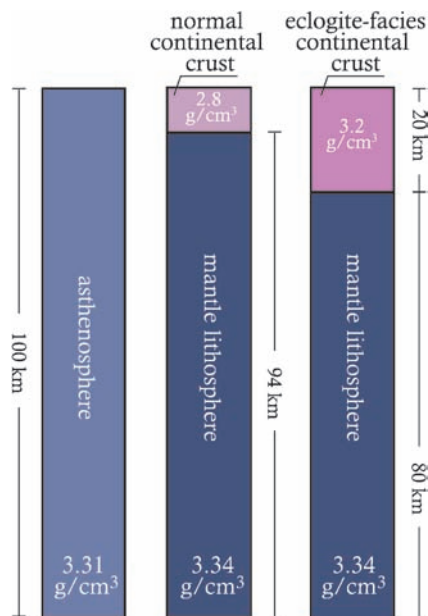


Fig. 11. A 100 km thick column of lithosphere with only 6 km of untransformed continental crust has the same mass as 100 km of asthenosphere; however, if the crust transforms to UHP minerals, the same 100 km thick lithosphere can be composed of 20 km of continental crust.

References

- Austrheim, H. (1987): Eclogitization of lower crustal granulites by fluid migration through shear zones. *Earth Planet. Sci. Lett.*, **81**, 221–232.
- (1998): The influence of fluid and deformation on metamorphism of the deep crust and consequences for geodynamics of collision zones. in “When Continents Collide: Geodynamics and Geochemistry of Ultrahigh-Pressure Rocks”, B.R. Hacker, and J.G. Liou, eds, Kluwer Academic Publishers, Dordrecht, p. 297–323.
- Austrheim, H., Erambert, M., Engvik, A.K. (1997): Processing of crust in the root of the Caledonian continental collision zone: the role of eclogitization. *Tectonophysics*, **273**, 129–153.
- Auzanneau, E., Vielzeuf, D., Schmidt, M.W. (2006): Experimental evidence of decompression melting during exhumation of subducted continental crust. *Contrib. Mineral. Petrol.*, **152**, 125–148.
- Banno, S., Enami, M., Hirajima, T., Ishiwatari, A., Wang, Q. (2000): Decompression *P-T* path of coesite eclogite to granulite from Weihai, eastern China. *Lithos*, **52**, 97–108.
- Baxter, E.F. (2003): Natural constraints on metamorphic reaction rates. in “Geochronology: Linking the Isotopic Record with Petrology and Textures”, D. Vance, W. Mueller, and I.M. Villa, eds., **220**, Geological Society of London Special Publication, p. 183–202.
- Baxter, E.F., Ague, J.J., DePaolo, D.J. (2002): Prograde temperature-time evolution in the Barrovian type-locality constrained by Sm/Nd garnet ages from Glen Clova, Scotland. *J. Geol. Soc. London*, **159**, 71–82.
- Bingen, B., Nordgulen, Ø., Viola, G. (2008): A four-phase model for the Sveconorwegian orogeny, SW Scandinavia. *Norwegian Journal of Geology*, **88**, 43–72.
- Black, P.M., Brothers, R.N., Yokoyama, K. (1988): Mineral paragenesis in eclogite-facies meta-acidites in northern New Caledonia. *Developments in Petrology*, **12**, 271–289.
- Bruceckner, H.K. & van Roermund, H.L.M. (2004): Dunk tectonics: a multiple subduction/duction model for the evolution of the Scandinavian Caledonides. *Tectonics*, **23**, doi: 10.10292003TC001502.
- Bryhni, I. (1966): Reconnaissance studies of gneisses, ultrabasites, eclogites and anorthosites in outer Nordfjord, Western Norway. *Norges geol. undersøkelse*, **241**, 1–68.
- Carlson, W.D. (2005): Intracrystalline diffusivities of REE, Y, V, and Cr in garnet at 700–900 degrees C. *Eos, Trans. Am. Geophys. Union*, **86**, Abstract V13A-0522.
- Carswell, D.A. & Cuthbert, S.J. (1986): Eclogite facies metamorphism in the lower continental crust. in “The Nature of the Lower Continental Crust”, J.B. Dawson, D.A. Carswell, J. Hall, and K.H. Wedepohl, eds., **24**, Blackwell Scientific Publications, Oxford p. 193–209.
- Carswell, D.A., Bruceckner, H.K., Cuthbert, S.J., Mehta, K., O’Brien, P.J. (2003a): The timing of stabilisation and the exhumation rate for ultra-high pressure rocks in the Western Gneiss Region of Norway. *J. Metamorphic Geol.*, **21**, 601–612.
- Carswell, D.A., Tucker, R.D., O’Brien, P.J., Krogh, T.E. (2003b): Coesite micro-inclusions and the U/Pb age of zircons from the Hareidland eclogite in the Western Gneiss Region of Norway. *Lithos*, **67**, 181–190.
- Cohen, A.S., O’Nions, R.K., Siegenthaler, R., and Griffin, W.L. (1988): Chronology of the pressure–temperature history recorded by a granulite terrain. *Contrib. Mineral. Petrol.*, **98**, 303–311.
- Cong, B., Zhai, M., Carswell, T.A., Wilson, R.N., Wang, Q., Zhao, Z., Windley, B.F. (1995): Petrogenesis of ultrahigh-pressure rocks and their country rocks at Shuanghe in Dabieshan, central China. *Eur. J. Mineral.*, **7**, 119–138.
- Connolly, J.A.D., and Petrini, K. (2002): An automated strategy for calculation of phase diagram sections and retrieval of rock properties as a function of physical conditions. *J. Metamorphic Geol.*, **20**, 697–798.
- Cuthbert, S.J., Carswell, D.A., Krogh-Ravna, E.J., Wain, A. (2000): Eclogites and eclogites in the Western Gneiss Region, Norwegian Caledonides. *Lithos*, **52**, 165–195.
- Dewey, J.F., Ryan, P.D., Andersen, T.B. (1993): Orogenic uplift and collapse, crustal thickness, fabrics and metamorphic phase changes; the role of eclogites. *Geological Society Special Publications*, **76**, 325–343.
- Dobrzhinetskaya, L.F., Eide, E.A., Larsen, R.B., Sturt, B.A., Tronnes, R.G., Smith, D.C., Taylor, W.R., Posukhova, T.V., Posukhova, T.V. (1995): Microdiamond in high-grade metamorphic rocks of the Western Gneiss region, Norway. *Geology*, **23**, 597–600.
- Dransfield, M. (1994): Extensional exhumation of high-grade metamorphic rocks in western Norway and the Zaskar Himalaya. University of Oxford, 225 p.
- Dutch, R. & Hand, M. (2009): Retention of Sm–Nd isotopic ages in garnets subjected to high-grade thermal reworking: implications for diffusion rates of major and rare earth elements and the Sm–Nd closure temperature in garnet. *Contrib. Mineral. Petrol.* 10 July 2009.
- Engvik, A.K., Austrheim, H., Andersen, T.B. (2000): Structural, mineralogical and petrophysical effects on deep crustal rocks of fluid-limited polymetamorphism, Western Gneiss Region, Norway. *J. Geol. Soc. London*, **157**, 121–134.
- Enkelmann, E., Ratschbacher, L., Jonckheere, R., Nestler, R., Fleischer, M., Gloaguen, R., Hacker, B.R., Zhang, Y.Q., Ma, Y.-S. (2006): Cenozoic exhumation and deformation of north-eastern Tibet and the Qinling: Is Tibetan lower crust flow diverging around the Sichuan Basin? *Geol. Soc. Am. Bull.*, **118**, 651–671.
- Ernst, W.G. (2001): Subduction, ultrahigh-pressure metamorphism, and reurgitation of buoyant crustal slices – implications for arcs and continental growth. *Phys. Earth. Planet. Inter.*, **127**, 253–275.
- (2006): Preservation/exhumation of ultrahigh-pressure subduction complexes. *Lithos*, **92**, 321–335.
- Gaál, G. & Gorbatshev, R. (1987): An Outline of the precambrian evolution of the baltic shield. *Precambrian Res.*, **35**, 15–52.
- Gee, D.G. (1975): A tectonic model for the central part of the Scandinavian Caledonides. *Am. J. Sci.*, **275-A**, 468–515.
- Gerya, T.V. & Stöckhert, B. (2006): Two-dimensional numerical modeling of tectonic and metamorphic histories at active continental margins. *Int. J. Earth Sci.*, **95**, 250–274.
- Gilotti, J.A. & Krogh Ravna, E. (2002): First evidence of ultrahigh-pressure metamorphism in the North-East Greenland Caledonides. *Geology*, **20**, 551–554.
- Glodny, J., Kühn, A., Austrheim, H. (2008): Diffusion versus recrystallization processes in Rb–Sr geochronology: Isotopic relics in eclogite facies rocks, Western Gneiss Region, Norway. *Geochim. Cosmochim. Acta*, **72**, 506–525.

- Hacker, B.R. (1996): Eclogite formation and the rheology, buoyancy, seismicity, and H₂O content of oceanic crust. in "Dynamics of Subduction", G.E. Bebout, Scholl, D., Kirby, S.H., Platt, J.P., eds., **96**, American Geophysical Union, Washington, D.C. p. 337–346.
- (2008): H₂O subduction beyond arcs. *Geochemistry Geophysics Geosystems*, **9**, Q03001, doi:10.1029/2007GC001707.
- Hacker, B.R. & Abers, G.A. (2004): Subduction Factory 3. An Excel worksheet and macro for calculating the densities, seismic wave speeds, and H₂O contents of minerals and rocks at pressure and temperature. *Geochemistry Geophysics Geosystems*, **5**, Q01005, doi: 10.1029/2003GC000614.
- Hacker, B.R. & Gans, P.B. (2005): Continental collisions and the creation of ultrahigh-pressure terranes: Petrology and thermochronology of nappes in the central Scandinavian Caledonides. *Geol. Soc. Am. Bull.*, **117**, 117–134.
- Hacker, B.R., Ratschbacher, L., Webb, L.E., Ireland, T.R., Calvert, A., Dong, S., Wenk, H.-R., Chateigner, D. (2000): Exhumation of ultrahigh-pressure continental crust in east-central China: Late Triassic–Early Jurassic tectonic unroofing. *J. Geophys. Res.*, **105**, 13339–13364.
- Hacker, B.R., Andersen, T.B., Root, D.B., Mehl, L., Mattinson, J.M., Wooden, J.L. (2003): Exhumation of high-pressure rocks beneath the Solund Basin, Western Gneiss Region of Norway. *J. Metamorphic Geol.*, **21**, 612–629.
- Hacker, B.R., Wallis, S.R., Ratschbacher, L., Grove, M., Gehrels, G.E. (2006): High-temperature geochronology constraints on the tectonic history and architecture of the ultrahigh-pressure Dabie-Sulu Orogen. *Tectonics*, **25**, doi:10.1029/2005TC001937.
- Harvey, J. & Baxter, E.F. (2009): An improved method for TIMS high precision neodymium isotope analysis of very small aliquots (1–10 ng). *Chem. Geol.*, **258**, 251–257.
- Heinrich, C.H. (1982): Kyanite-eclogite to amphibolite facies evolution of hydrous mafic and pelitic rocks, Adula nappe, central Alps. *Contrib. Mineral. Petrol.*, **81**, 30–38.
- Holler, R.A., & Stowell, H.H. (2008): Use of Phase Diagram Sections to Constrain the *P-T* of Garnet Porphyroblast Growth in Amphibolite: An Example from the Nason Ridge Migmatitic Gneiss, WA. *Geol. Soc. Am., Abstr with Programs*, **40**, 516.
- John, T. & Schenk, V. (2003): Partial eclogitisation of gabbroic rocks in a late Precambrian subduction zone (Zambia): prograde metamorphism triggered by fluid infiltration. *Contrib. Mineral. Petrol.*, **146**, 147–191.
- Johnson, D.M., Hooper, P.R., Conrey, R.M. (1999): XRF analysis of rocks and minerals for major and trace elements on a single low dilution Li-tetaborate based bead. *Adv. X-ray anal.*, **41**, 843–867.
- Knaak, C.S.C. & Hooper, P.R. (1994): Trace element analysis of rocks and minerals by IC-PMS. Geoanalytical Laboratory. *Wash. State Univ.*, **2.0**, 18.
- Kohn, M.J. & Spear, F. (2000): Retrograde net transfer reaction insurance for pressure-temperature estimates. *Geology*, **28**, 1127–1130.
- Koons, P.O., Rubie, D.C., Frueh-Green, G. (1987): The effects of disequilibrium and deformation on the mineralogical evolution of quartz diorite during metamorphism in the eclogite facies. *J. Petrol.*, **28**, 679–700.
- Krabbendam, M., Wain, A., Andersen, T.B. (2000): Pre-Caledonian granulite and gabbro enclaves in the Western Gneiss Region, Norway: indications of incomplete transition at high pressure. *Geological Magazine*, **137**, 235–255.
- Kretz, R. (1983): Symbols for rock-forming minerals. *Am. Mineral.*, **68**, 277–279.
- Krogh, T., Kwok, Y., Robinson, P., Terry, M.P. (2004): U-Pb constraints on the subduction-extension interval in the Averøya-Nordøyane area, Western Gneiss Region, Norway. *Goldschmidt Conference Abstract*.
- Kylander-Clark, A.R., Hacker, B.R., Corfu, F. (2006): Large-Scale, Short-Lived Subduction of the Western Gneiss Region Ultrahigh-Pressure Terrane. *Eos, Trans Am Geophys Union*, **87**, Abstract T53C-1619.
- Kylander-Clark, A.R.C., Hacker, B.R., Johnson, C.M., Beard, B.L., Mahlen, N.J., Lapen, T.J. (2007): Coupled Lu–Hf and Sm–Nd geochronology constrains prograde and exhumation histories of high- and ultrahigh-pressure eclogites from western Norway. *Chem. Geol.*, **242**, 137–154.
- Kylander-Clark, A.R.C., Hacker, B.R., and Mattinson, J.M. (2008): Slow exhumation of UHP terranes: Titanite and rutile ages of the Western Gneiss Region, Norway. *Earth Planet. Sci. Lett.*, **272**, 531–540.
- Labrousse, L., Jolivet, L., Andersen, T.B., Agard, P., Maluski, H., Schärer, U. (2004): Pressure-temperature-time-deformation history of the exhumation of ultra-high pressure rocks in the Western Gneiss region, Norway. *Geol. Soc. Am. Spec. Pap.*, **380**, 155–185.
- Lapen, T.J., Johnson, C.M., Baumgartner, L.P., Mahlen, N.J., Beard, B.L., Amato, J.M. (2003): Burial rates during prograde metamorphism of an ultra-high-pressure terrane; an example from Lago di Cignana, Western Alps, Italy. *Earth Planet. Sci. Lett.*, **215**, 57–72.
- Lenze, A. & Stöckhert, B. (2007): Microfabrics of UHP metamorphic granites in the Dora Maira Massif, western Alps – no evidence of deformation at great depth. *J. Metamorph. Geol.*, **25**, 461–475.
- Liu, J. & Liou, J.G. (1995): Kyanite anthophyllite schist and the southwest extension of the Dabie Mountains ultrahigh to high pressure belt. *Island Arc*, **4**, 334–346.
- Ludwig, K. (2003): Isoplot 3.00. Berkeley Geochronology Center Special Publication, **4**, p. 70.
- Mahar, E.M., Baker, J.M., Powell, R., Holland, T.J.B., Howell, N. (1997): The effect of Mn on mineral stability in metapelites. *J. Metamorphic Geol.*, **15**, 223–238.
- Massonne, H.J. (2008): Hydration, dehydration, and melting of upper crustal rocks at high pressure and ultrahigh pressure conditions. *International Geological Congress*, **33**, Abstract 1320309.
- Mattinson, C.G., Menold, C.A., Zhang, J.X., Bird, D.K. (2007): High- and Ultrahigh-Pressure Metamorphism in the North Qaidam and South Altyn Terranes, Western China. *International Geology Review*, **49**, 969–995.
- McClelland, W.C., Power, S.E., Gilotti, J.A., Mazdab, F.K., and / addinfo> Wopenka, B. (2006): U-Pb SHRIMP geochronology and trace-element geochemistry of coesite-bearing zircons, north-east Greenland Caledonides. *Geol. Soc. Am. Spec. Pap.*, **403**, 22–43.
- Mearns, E.W. (1986): Sm-Nd ages for Norwegian garnet peridotite. *Lithos*, **19**, 269–278.
- Nakamura, D. & Hirajima, T. (2000): Granulite-facies overprinting of ultrahigh-pressure metamorphic rocks, northeastern Sulu region, eastern China. *J. Petrol.*, **41**, 563–582.
- Okay, A.I. (1993): Petrology of a diamond and coesite-bearing metamorphic terrain: Dabie Shan, China. *Eur. J. Mineral.*, **5**, 659–675.

- Powell, R. & Holland, T.J.B. (1988): An internally consistent dataset with uncertainties and correlations: 3. Applications to geobarometry, worked examples and a computer program. *J. Metamorphic Geol.*, **6**, 173–204.
- Root, D.B., Hacker, B.R., Gans, P., Eide, E., Ducea, M., Mosenfelder, J. (2005): Discrete ultrahigh-pressure domains in the Western Gneiss Region, Norway; implications for formation and exhumation. *J. Metamorphic Geol.*, **23**, 45–61.
- Root, D.B., Hacker, B.R., Mattinson, J.M., and Wooden, J.L. (2004): Young age and rapid exhumation of Norwegian ultrahigh-pressure rocks: an ion microprobe and chemical abrasion study. *Earth Planet. Sci. Lett.*, **228**, 325–341.
- Rubie, D.C. (1986): The catalysis of mineral reactions by water and restrictions on the presence of aqueous fluid during metamorphism. *Mineral. Mag.*, **50**, 399–415.
- Schärer, U. & Labrousse, L. (2003): Dating the exhumation of UHP rocks and associated crustal melting in the Norwegian Caledonides. *Contrib. Mineral. Petrol.*, **144**, 758–770.
- Skora, S., Baumgartner, L.P., Mahlen, N.J., Johnson, C.M., Hellebrand, E. (2006): Diffusion-limited REE uptake by eclogite garnets and its consequences for Lu/Hf and Sm/Nd geochronology. *Contrib. Mineral. Petrol.*, **152**, 703–720.
- Spear, F.S., Kohn, M.J. (1996): Trace element zoning in garnet as a monitor of crustal melting. *Geology*, **24**, 1099–1102.
- Spengler, D., Brueckner, H.K., van Roermund, H.L.M., Drury, M.R., Mason, P.R.D. (2009): Long-lived, cold burial of Baltica to 200 km depth. *Earth Planet. Sci. Lett.*, **281**, 27–35.
- Straume, Å.K. & Austrheim, H. (1999): Importance of fracturing during retro-metamorphism of eclogites. *J. Metamorphic Geol.*, **17**, 637–652.
- Tabata, H., Yamauchi, K., Maruyama, S., Liou, J.G. (1998): Tracing the extent of a UHP metamorphic terrane: A mineral-inclusion study of zircons in gneisses from the Dabie Shan. in “When Continents Collide: Geodynamics and Geochemistry of Ultrahigh-Pressure Rocks”, B.R. Hacker, and J.G. Liou, eds, Kluwer Academic Publishers, Dordrecht, p. 261–274.
- Terry, M.P. & Heidelbach, F. (2006): Deformation-enhanced metamorphic reactions and the rheology of high-pressure shear zones, Western Gneiss Region, Norway. *J. Metamorphic Geol.*, **24**, 3–18.
- Terry, M.P., Robinson, P., Hamilton, M.A., Jercinovic, M.J. (2000): Monazite geochronology of UHP and HP metamorphism, deformation, and exhumation, Nordøyane, Western Gneiss Region, Norway. *Am. Mineral.*, **85**, 1651–1664.
- Tirone, M., Ganguly, J., Dohmen, R., Langenhorst, F., Hervig, R., Becker, H.-W. (2005): Rare earth diffusion kinetics in garnet; experimental studies and applications. *Geochim. Cosmochim. Acta*, **69**, 2385–2398.
- Vielzeuf, D. & Holloway, J.R. (1988): Experimental determination of the fluid-absent melting relations in the pelitic system. Consequences for crustal differentiation. *Contrib. Mineral. Petrol.*, **98**, 257–276.
- Wain, A. (1997): New evidence for coesite in eclogite and gneisses; defining an ultrahigh-pressure province in the Western Gneiss region of Norway. *Geology*, **25**, 927–930.
- Wain, A., Waters, D., Austrheim, H. (2001): Metastability of granulites and processes of eclogitization in the UHP region of western Norway. *J. Metamorphic Geol.*, **19**, 609–625.
- Walsh, E.O. & Hacker, B.R. (2004): The fate of subducted continental margins: Two-stage exhumation of the high-pressure to ultrahigh-pressure Western Gneiss complex, Norway. *J. Metamorphic Geol.*, **22**, 671–689.
- Wang, X. & Liou, J.G. (1991): Regional ultrahigh-pressure coesite-bearing eclogitic terrane in central China: evidence from country rocks, gneiss, marble, and metapelite. *Geology*, **19**, 933–936.
- Wang, X., Liou, J.G., Maruyama, S. (1992): Coesite-bearing eclogite from the Dabie Mountains, central China: Petrology and *P-T* path. *J. Geol.*, **100**, 231–250.
- Warren, C.J., Beaumont, C., Jamieson, R.A. (2008a): Formation and exhumation of ultra-high-pressure rocks during continental collision: Role of detachment in the subduction channel. *Geochem. Geophys. Geosystems*, **9**, Q04019, doi:10.1029/2007GC001839.
- , —, —, (2008b): Modelling tectonic styles and ultra-high pressure (UHP) rock exhumation during the transition from oceanic subduction to continental collision. *Earth Planet. Sci. Lett.*, **267**, 129–145.
- Wilks, S.J. & Cuthbert, S.J. (1994): The evolution of the Hornelen Basin detachment system, western Norway: implications for the style of late orogenic extension in the southern Scandinavian Caledonides. *Tectonophysics*, **238**, 1–30.
- Yamato, P., Burov, E., Agard, P., Le Pourhiet, L., Jolivet, L. (2008): HP-UHP exhumation during slow continental subduction: Self-consistent thermodynamically and thermomechanically coupled model with application to the Western Alps. *Earth Planet. Sci. Lett.*, **271**, 63–74.
- Young, D.J., Hacker, B.R., Andersen, T.B., Corfu, F., Gehrels, G.E., Grove, M. (2007): Amphibolite to ultrahigh-pressure transition in western Norway: Implications for exhumation tectonics. *Tectonics*, **26**, doi:10.1029/2004TC001781.
- Zhang, R., Liou, J.G., Ernst, W.G. (1995): Ultrahigh-pressure pressure metamorphism and decompressional *P-T* paths of eclogites and country rocks from Weihai, eastern China. *Island Arc*, **4**, 293–309.

Received 14 January 2009

Modified version received 27 August 2009

Accepted 22 September 2009